IEEE Access
Multidisciplinary | Rapid Review | Open Access Journal

Received 11 December 2024, accepted 31 December 2024, date of publication 3 January 2025, date of current version 9 January 2025.

Digital Object Identifier 10.1109/ACCESS.2025.3525999

RESEARCH ARTICLE

Real Time Fractional Robust Adaptive Scheme for Frequency Regulation in Double Area Hybrid Power System With Renewables

AHMED RAGAB[1], DALIA ALLAM[2], AHMED F. ZOBAA[3], (Senior Member, IEEE), AND HAZEM ALI ATTIA[1]

[1]Engineering Mathematics and Physics Department, Faculty of Engineering, Fayoum University, Faiyum 63514, Egypt
[2]Electrical Engineering Department, Faculty of Engineering, Fayoum University, Faiyum 63514, Egypt
[3]College of Engineering, Design and Physical Science, Brunel University of London, UB8 3PH Uxbridge, U.K.

Corresponding author: Ahmed F. Zobaa (azobaa@ieee.org)

ABSTRACT Load frequency regulation in hybrid grid is a very crucial issue. This work introduces robust-adaptive control methodology to provide accurate response against any disturbances. Control scheme of two main parts has been introduced. The first one is a novel fractional order model reference adaptive controller where fractional calculus merits and e-modification robust algorithm have been merged with the adaptive skills creating the fractional order model reference robust-adaptive controller. This robust-adaptive controller has utilized output feedback approach that requires only the output state without detailed system model information. The fractional orders have been optimized using a nature-inspired algorithm named Artificial Rabbits. The second part of the control scheme is a disturbance rejection observer that is able to estimate and eliminate external and internal disturbances. For fair comparison, results of the proposed scheme have been compared to that of the most efficient controllers obtained from the literature named fractional order proportional integral derivative controller and integral controller. Furthermore, the integer version of the proposed controller has been tested and compared with the proposed controller to prove the robustness of the fractional modification. To validate the superiority of the proposed controller, five challenging scenarios have been considered, encompassing load fluctuations, integration of renewable energy sources, changes in system parameters and time delay attacks. The proposed controller effectively minimizes area control error achieving stability and showing cost function enhancement of 15% to 152% compared to other tested controllers in all scenarios. Thus, it is strongly recommended for load frequency regulation in multi-area power systems.

INDEX TERMS Adaptive model reference control, disturbance rejection, fractional control, frequency regulation, renewable resources.

I. INTRODUCTION

The heightened intricacy of modern power systems, along with emerging uncertainties and environmental restrictions, underscores the significance of load frequency control (LFC). This function, a key component of automatic generation control (AGC), has become pivotal in ensuring power system stability and averting blackouts. Power system stability refers to the grid's capacity to sustain its nominal equilibrium despite disturbances or uncertainties [1]. Frequency instability, a manifestation of power system instability, often arises from significant mismatches between generation and demand, leading to deviations from the nominal frequency [2]. Significant frequency deviation poses a critical concern, as it can trigger adverse effects on the power system, including equipment damage, transmission line overload, and disruptions to protection schemes [3]. Therefore, load frequency control (LFC) is essential for maintaining the

The associate editor coordinating the review of this manuscript and approving it for publication was Nga Nguyen.

nominal frequency and planned tie line power among interconnected areas, thus mitigating the destructive consequences of frequency deviation.

In a typical dynamic power system, active elements are interconnected via tie lines to deliver power to varying loads, which introduces dynamic and random fluctuations that can deviate the frequency from its nominal value [4]. The substantial inertia of traditional synchronous generators contributes to the system's inertia constant, bolstering frequency stability [5]. However, the increasing integration of renewable energy sources (RES) introduces uncertainties that challenge LFC performance. RES such as wind farms and photovoltaic (PV) panels, characterized by low inertia and connection via power converters, diminish the system's inertia constant, thereby posing a threat to frequency stability [6]. Consequently, there's a pressing need for more flexible, robust controllers, and advanced computational techniques in LFC algorithms [6].

Various power system configurations, incorporating nonlinearities, have been investigated to address frequency stability concerns. These include individual systems [7], [8], multiple-region electrical systems as Four-Area system [9] and Three-Area system [10], [11] and non-regulated power grids [12], [13]. To maintain the frequency within acceptable limits, a variety of controllers and algorithms are utilized. The PID controller stands out as the most prevalent conventional controller in the industry, owing to its simplicity. Consequently, it can be effectively employed for grid frequency and tie line power control purposes. Additionally, various modifications and configurations can be applied to enhance the performance of the PID controller. For instance, in [14], the study explored AGC employing a double-mode PI controller, aiming for improved control effectiveness. In LFC within the time domain, the performance analysis involved the utilization of controllers such as Integral with Double Derivative (IDD), as well as Integral (I), Proportional-Integral (PI), Integral-Derivative (ID), and Proportional-Integral-Derivative (PID) controllers [15]. In [16], a PID controller with a derivative filter was employed to regulate the grid frequency in a triple area conventional power network. In [17], a distributed fault-tolerant PI controller based on a stochastic event-triggered scheme is proposed for the purpose of load frequency control in a multi-area power system.

MPC (Model Predictive Controller) is an advanced control technique that predicts and optimizes the future behavior of the controlled system by sequentially computing manipulated variables [18], [19]. Distributed MPC based on Laguerre series function has shown superiority as load frequency regulator in comparison with other classic controllers [20]. Model predictive LFC was introduced in [21], considering the network structure and power exchange in tie-lines. In [22], the response of power system frequency regulation was enhanced with the incorporation of a wind energy source, achieved through the design of an analytical linearized model for frequency characteristics while utilizing a load frequency MPC controller.

Optimal control methods have also been utilized in the literature to support power system frequency regulation. These techniques often surpass classic PID regulators, which face challenges in parameter setting and maintaining stability with the existence of system uncertainties. One such controller is the linear quadratic regulator (LQR), which has been employed to enhance load frequency control in interconnected power systems. In [23], LQR with a link to a Kalman filter was used as a secondary control to enhance system frequency in interconnected power systems. Additionally, LQR has been applied in a grid comprising a multi-area power system with dynamics were expressed in state space form to bolster the frequency of the system [24].

Disturbances represent the most prevalent factors impacting the desired performance of physical systems. Leveraging disturbance observers to swiftly estimate these disturbances and executing disturbance cancellation through the controller stands out as a valuable technique in addressing these challenges [25]. Adding a disturbance observer to the supplementary loop that has TID (Tilt Integral Derivative) controller enhanced the performance of the load frequency control in conventional multiple-area systems [26]. In [27], a disturbance estimation controller was utilized to attain frequency and tie line power stability in a multi-area AC/DC hybrid system following demand power mismatches. In [28], a combination of disturbance observer and sliding mode controller was utilized to execute load frequency regulation within a microgrid featuring renewable energy resources.

The widespread application of fractional calculus across various engineering domains has significantly expanded, driven by enhanced performance, increased flexibility, additional degrees of freedom offered by fractional controllers, and improved accuracy. Consequently, researchers have shown a growing interest in fractional controllers [29]. As a result of the uncertain nature and nonlinearities inherent in power systems, the demand for more robust controllers, such as fractional controllers, is on the rise. A conventional single-area system was controlled by load frequency FOPID regulator in [30] and enhancement was shown versus integer PID. In order to identify levels of parameters variation, Kharitonov's theorem was used in [31] to design FOPID controller for interval model single-area power system. In [32], IMC (Internal Model Control) based fractional order PID with fractional order filter and reduced order module was used to regulate frequency in multi-area system during load perturbation. Due to the merits of the TID controllers over the classical FOPID controllers such as the increased robustness and the superior effectiveness in mitigating disturbances versus classical fractional order PID controllers, they were employed in [33] and [34] to improve the performance of the LFCs in single and multi-area power systems. In [35], the FOPID controller was optimized using the Artificial Gorilla Troops algorithm to function as a supplementary load

TABLE 1. Comparison between some existing studies in literature and the proposed study.

Ref	Supplementary Regulator Scheme	Adaptive ?	Adaptive Scheme	Power System Construction	Renewables Included?	Comparison Metric
[7]	PIDA (Proportional Integral Derivative Acceleration) Tunned by Pole Placement	No	×	Conventional Single-Area, Two-Area and Four-Area Power Systems without Renewables	No	Frequency Overshoots and Settling Time
[8]	PID Controller with Parameters Obtained by Laurant Series Expansion	No	×	Conventional Single-Area and Four-Area Power System	No	Frequency Overshoots and Settling Time
[9]	Multi-Agent Reinforced Learnt Controller with Particle Swarm Optimized Gains	No	×	Conventional Four-Area Power System	No	Mean Square Errors of System States
[10]	Fuzzy Logic PID	No	×	Conventional Three-Area Power System	No	Maximum Deviation and Settling Time
[11]	Non-Linear Sliding Mode	No	×	Conventional Three-Area Power System	No	ITAE (Integral Time Square Error)
[12]	Fuzzy Logic PI Control	No	×	Conventional Two-Area Power System Integrated with Wind Energy	Yes; Wind Energy	ISE (Integral Square Error)
[13]	IMC-PID (Internal Mode Control with PID)	No	×	Conventional Four-Area Power System	No	Maximum Deviation
[14]	Dual Mode PI Controller Tunned by Hooke-Jeeve Optimizer	No	×	Conventional Two-Area Power System	No	ISE
[16]	PID Controller with Derivative Filter (PIDF)	No	×	Conventional Three-Area Power System	No	ITAE
[17]	Fault Tolerant PI Control Strategy	No	×	Conventional Single-Area and Two-Area Power System	No	Frequency Deviation
[19]	MPC (Mode Predictive Control) optimized by Bat Inspired Algorithm	No	×	Conventional Two-Area Power System	No	ISE
[20]	Distributed MPC	No	×	Conventional Two-Area and Three-Area Power System	No	Orthonormal Laguerre Function Expansion
[21]	Neural Network MPC with Levenberg–Marquardt optimization	No	×	Conventional Two-Area Power System	No	Quadratic Formula of ACE
[22]	MPC	No	×	Conventional Three-Area Power System Integrated with Wind Farms	Yes; Wind Energy	Quadratic Formula of Deviations in Frequency and Tie-Line Power
[23]	LQR (Linear Quadratic Regulator) with Kalman Filter	No	×	Conventional Two-Area Power System	No	Optimal Control Problem Using Quadratic Form of System States
[24]	Distributed LQR with Convex Optimization	No	×	Conventional Six-Area Power System	No	Convex Combination of Hurwitz Matrices
[26]	TID (Tilt-Integral-Derivative) Controller Equipped with Disturbance Observer	No	×	Conventional Two-Area and Three-Area and Five-Area Power System Integrated with Wind Farms	Yes; Wind Energy	ISE
[27]	Disturbance Rejection Based Controller	No	×	Conventional Three-Area Power System	No	Root Mean Square of Frequency Deviations
[28]	Double Sliding Mode Control	Yes	Adaptive Sliding Mode Through Disturbance Observer	Conventional One-Area System with PV and Wind Farm	Yes; Wind Energy and PV	Frequency Deviation
[30]	Fractional Order PID Controller (FOPID)	No	×	Conventional Single-Area Power System	No	IAE (Integral Absolute Error), ISE and ITAE
[31]	Kharitonov's theorem Based FOPID Controller	No	×	Conventional Single-Area Power System	No	IAE, ISE and ITAE
[32]	IMC-FOPID Controller	No	×	Conventional Single-Area and Two-Area Power System	No	IAE, ISE and ITAE
[34]	Hybrid FOPID-TID Controller	No	×	Conventional Two-Area System with PV and Wind Farm	Yes; Wind Energy and PV	ISE
[35]	FOPID Optimized by Artificial Gorilla Troops	No	×	Conventional Two-Area System	No	Frequency Deviation and Error Cost Function
[36]	Direct-Indirect Adaptive Fuzzy Controller	Yes	Approximation of System Parameters Using Fuzzy Rules and H_∞ Tracking	Conventional Three-Area Power System	No	ITAE
[37]	Reduced Order State Model Adaptive Control	Yes	Signal Synthesis Adaptation to Eliminate Sensitivity to System Changes	Conventional Two-Area Power System	No	Frequency Deviation
[38]	Multi-Level Adaptive Self Tunning Regulator	Yes	Parameters Estimation Using Recursive Least Squares	Conventional Multi-Area Power System	No	Frequency Deviation
[39]	PID Controller Tuned by Particle Swarm and Combined with adaptive virtual inertia loop	Yes	Adjustment of Virtual Inertia Loop Gains by Fuzzy Platform	Conventional Single Area Connected with Microgrid of Wind Turbines and PV Panels	Yes; Wind Energy and PV	ISE
Proposed Work	**Fractional Robust-Adaptive Controller Combined with Disturbance Rejection Observer**	**Yes**	**Fractional Model Reference Adaptive Lyapunov Output Feedback Approach Merged with Robust e-modification**	**Conventional Two-Area Power System with PV and Wind Farm**	**Yes; Wind Energy and PV**	**ITSE (Integral Time Square Error)**

frequency regulator in a two-area interconnected power system. Its performance was benchmarked against four advanced metaheuristic techniques, demonstrating its superior effectiveness.

Adaptive controllers represent promising devices that differ from robust controllers in their approach to operation. Unlike robust controllers, which assume worst-case conditions, adaptive controllers aim to minimize deviations from the desired response by continuously estimating system uncertainties online and generating the necessary control action accordingly [40]. The approaches of self-adjustable regulators can be categorized to adaptive gain coordinating, reference framework, self-adjusting regulator, and two-mode control [41]. Model-based adaptive systems generate a control signal in such a way that the controlled system tracks the output of a model reference system while ensuring stability is maintained [42]. Various schemes, such as output feedback schemes and state space representations, have been proposed for Model Reference Adaptive Control (MRAC) techniques. These schemes involve designing model reference and adaptive laws, such as the MIT law and Lyapunov law [43].

Merging of fractional calculus in the control theory allows for the utilization of fractional adaptive laws in MRAC. This substitution of classical adaptive laws with fractional adaptive laws has demonstrated improved performance in model reference tracking [44]. In [39], PID controller was used as supplementary regulator while a synthetic adaptive with fuzzy platform identification algorithm was utilized for inertia control in an interconnected grid merged with renewables. In [45], an adaptive controller was employed as a LFC device in a multi-area power system devoid of RES to meet the hyper-stability condition. Remarkably, this adaptive controller only required information pertaining to output and available states, eliminating the necessity to know specific system parameters. A Direct-Indirect adaptive fuzzy control approach was utilized to formulate a fuzzy adaptive control law with a parameters estimation algorithm for LFC in a multi-area power system [36]. Various adaptive control approaches were employed in [37], [38], [40], and [41], including self-adjusting regulators, tiered adaptive strategies, and compact variable frameworks, to contribute to LFC in multiple zone systems, both with including and excluding RESs. In [46], a control methodology based on the estimation of system inertia using recursive least squares is proposed for online LFC of a multi-area power system integrated with renewable energy sources. In [47], the control process has been tackled with the virtual inertia process at the moment of renewables connection to control the feedforward gain of the virtual inertia where the adaptive control signal has been proportional to the desired reference. In [47], the virtual inertia controller approach is designed using both of a fractional model reference and a fractional adaptation process and the secondary control has been accomplished via (FOID – P) controller.

The integration of renewable energy sources and increasing complexity in power systems introduce significant uncertainties in system parameters, necessitating the adoption of advanced control strategies. Developing precise mathematical models for these systems that incorporate all relevant parameters remains a formidable challenge. Model reference adaptive controllers (MRACs), which operate without relying on detailed plant models, provide an effective solution for addressing such uncertainties. By continuously adjusting controller parameters in real time to counteract disturbances, MRACs can significantly enhance system performance. Given the limited studies on model reference adaptive load frequency controllers in the literature, as shown in Table 1, further research is urgently needed to develop robust MRAC-based supplementary online control strategies for hybrid multi-area power systems.

Therefore, this work proposes a novel adaptive output feedback control scheme with a disturbance rejection methodology for secondary loop control in a double area power system to regulate the frequency during the load variations and the internal or the external disturbances. The adaptive controller approach includes an integer order reference model, fractional order adaptation skills and a robust modification in the adaptive process via e-modification algorithm. The adaptive controller parameters in this work are not only the feedforward gains as in [47] but also the feedback gains and the auxiliary gains where, the auxiliary states have been created by the auxiliary generator of the controller. The adaptive control signal is a linear combination of the auxiliary stats, the set point and the measured output. More details about the new contributions of this paper are as follows:

1- Proposing an online model reference adaptive control scheme to manage frequency variations in a power system with renewables. It addresses challenges like severe load perturbations, parameters change and reduced system inertia caused by semi-conductive converters in renewable plants. The scheme ensures robust adaptive and efficient frequency regulation despite these complexities.
2- Merging the merits of the fractional calculus with the adaptation skills of the adaptive model reference controller have been accomplished and tested based on Lyapunov stability theory providing an effective adaptive control for any change of the frequency. The fractional adaptive equations provide an improved response and better efficiency by adding extra degrees of freedom and improve the controller behavior.
3- The proposed control scheme employs closed-loop feedback by measuring the system's output and creating auxiliary states. It dynamically adjusts controller parameters online through adaptive differential equations and a reference model, ensuring effective adaptive control. The study compares integer and fractional adaptive equations, demonstrating the superior performance of the fractional approach.

4- Improving the robustness of the adaptive controller by incorporating e-modification robust algorithm into the Lyapunov based MRAC to eliminate the difficulties of the parameters drift and to enhance the robustness of the proposed controller.
5- Providing a disturbance rejection scheme in the proposed controller via a prober estimation of the disturbances using a disturbance observer design to improve its performance during any change in the frequency in response to load variation, sever system parameters changes and reconfiguration of power system via adding renewables as well.
6- Optimizing the fractional order of the fractional adaptive equations via a nature inspired optimization algorithm named rabbit artificial optimizer [48].
7- To further validate the proposed scheme, the recently introduced FOPID controller was implemented and optimized using the Artificial Rabbits Algorithm [48] to estimate its optimal parameters. The results were compared with the proposed scheme to demonstrate its superior performance. Additionally, an integral controller (IC) was tested, and its performance was compared to that of the proposed controller. These comparisons highlight the proposed scheme's effectiveness over existing controllers.
8- Five scenarios have been investigated to prove the efficiency and the robustness of the proposed control scheme, the first one tests the performance of FOMRAC controller w.r.t. that of FOPID, IC and IOMRAC at a certain load disturbance. The second scenario examines the FOMRAC fulfillment at severe load disturbances and compares its results with the other controllers. The third one investigates the achievements of the proposed controller upon the reconfiguration of the power system via insertion of various types of renewables and compares the results with these of FOPID and IOMRAC. The fourth one emulates the behavior of FOMRAC as well as IOMRAC and FOPID against the problem of the time delay attacks. The last scenario compares the performance of the proposed controller with the other controllers in the presence of severe system parameters changes. It is worth noting that the proposed FOMRAC control scheme proves its outstanding performance in stabilizing the system frequency with the lowest integral time squared error (ITSE).
9- The proposed control scheme offers online adaptation during severe load disturbances, significant system parameter changes, and power system reconfiguration with the integration of renewables. Unlike other controllers, it does not require retuning its parameters. Additionally, it achieves optimal performance based solely on output measurements, making it highly efficient for load frequency control. This flexibility and performance make the proposed scheme the best option for load frequency regulation.

II. POWER SYSTEM MODELING FOR LFC

This study focuses on LFC in a two-area power system, exploring LFC strategies for conventional power resources both with and without RESs, specifically solar and wind power. As documented in the literature, the aim of LFC methodologies is to mitigate frequency and tie line power deviations in interconnected power systems, particularly those resulting from high RESs penetration and random load disturbances. The main controlled variable in the interconnected power system is the error of area control (ACE), which combines the power system frequency and tie line power in a linear fashion [5]. The primary frequency control action aims to counteract the impact of disturbances on the system frequency by utilizing the stored kinetic energy of rotating parts. However, this primary control may not always be sufficient to restore the system to its rated frequency and scheduled tie line power. Therefore, supplementary secondary control becomes necessary. The target of the supplementary LFC controller is to minimize the ACE as much as possible, ensuring that the scheduled power system frequency and tie line power are maintained [49]. A linear simplified frequency response representation for the generator-demand dynamic (as illustrated in Fig. 1) describing the relationship between the incremental power mismatch and the frequency deviation can be expressed both in the time domain and the frequency domain as follows [5]:

$$\Delta P_{m_i}(t) - \Delta P_{L_i}(t) = 2H_i \frac{d\Delta f_i(t)}{dt} + D_i \Delta f_i(t) \quad (1)$$

$$\frac{\Delta f_i(s)}{\Delta P_{m_i}(s) - \Delta P_{L_i}(s)} = \frac{1}{D_i + 2H_i s}. \quad (2)$$

where ΔP_m is the turbine output power change in pu, ΔP_L is the demand change, H is constant of inertia, D is the damping factor and the lower index in $(\cdot)_i$ indicates the specification of i^{th} area. Conventional plants are equipped with speed governors and turbines to maintain their synchronous generators at synchronous speed. Models for speed governors and turbines, suitable for LFC analysis, can be represented as first-order systems, as follows [5]:

$$G_g = \frac{1}{1 + T_g s} \quad (3)$$

$$G_t = \frac{1}{1 + T_t s}. \quad (4)$$

The two main processes of the inertial LFC are the primary (droop) loop and supplementary loop. During the disturbance and frequency deviation, traditional stations can reinforce the system through the kinetic energy form their synchronous generators. This first inertial action is the primary control and can be activated by the droop characteristics of the generators. The final frequency deviation that can be calculated by (5) settles down the nominal value. Also, the tie line powers are

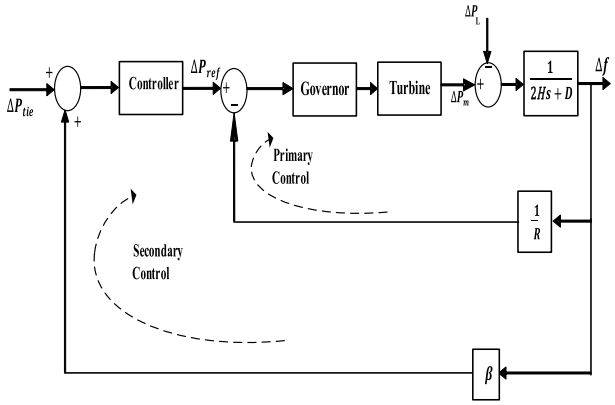

FIGURE 1. Building control block diagram of LFC methodology.

expected to deviates from the scheduled.

$$\Delta f_i = -R_i \Delta P_{L_i}. \tag{5}$$

where R is the droop coefficient in Hz/pu. As shown in previous paragraph, the performance of the primary control can stabilize the frequency that may be at a value that is different from nominal so, the secondary control is added to retain the nominal frequency and tie line power by changing the reference power to the governor-turbine block via suitable controller [50]. A suitable linear combination in (6) that creates the ACE signal can be considered as a good indication to the power imbalance in each area [5].

$$ACE_i = \Delta P_{tie,i} + \beta_i \Delta f_i. \tag{6}$$

where ACE_i is the area control error of area i, $\Delta P_{tie,i}$ is the change in tie line power of area i, Δf_i is the frequency deviation of the area i and β_i is a bias value of area i.

As illustrated in Fig. 2, the power system of study is composed of two control areas with PV plant is connected to area-1 and wind farm is connected to area-2. Each control area of the 2-area interconnected power system comprises a thermal power plant with reheat cycle, hydropower plant and gas turbine power station. All signals that can be measured and transmitted to the regulators and control centers are possible nodes of cyber-attacks as shown in [51]. Every single area produces 2000 MW rated output power and has a nominal load of 1740 MW. Generation Rate Constraint (GRC) and Governor Dead Band (GDB) are nonlinearities that are presented in the conventional power systems which is considered in this work as reasons that can affect the performance of the LFC. GRC for increasing and decreasing rates can be considered as 10% per minutes (0.0017 pu.MW/s) for the thermal power plant and 270% per minutes (0.045 pu.MW/s) increasing rate and 360% per minutes (0.06 pu.MW/s) decreasing rate for the hydropower plant respectively. The mathematical model of the conventional 2-area power system is illustrated in Fig. 3 with values of system parameters are shown in [52].

A. WIND POWER PLANT MODEL FOR LFC

Wind energy is one of the common RESs of electric power which is dependent on the random speed of the wind. The wind power plant model can be developed by employing the random white-noise source in MATLAB/Simulink to replicate the variability of wind speed, as demonstrated in Fig. 4 [53]. The rated output wind power can be calculated by:

$$P_w = 0.5 \rho A_T V_w^3 C_p(\lambda, \beta). \tag{7}$$

where ρ is the air density (kg/m^3), A_T is the rotor swept area (m^2) and C_p is the power coefficient of the wind turbine blades. The output power profile of the studied wind power plant model is shown in Fig. 5.

B. SOLAR POWER MODEL FOR LFC

The power output of the PV plant is irregular due to the dependence on the weather conditions as the solar irradiance and the temperature which may make the output fluctuates causing large frequency and voltage deviations. Fluctuations of PV output can be modeled as in Fig. 6 using white noise signal multiplied by uniform and nonuniform insolation [54]. Equation that can emulate the actual solar output power deviation is reviewed from [54]. The output power profile of the studied PV plant model is illustrated in Fig. 7.

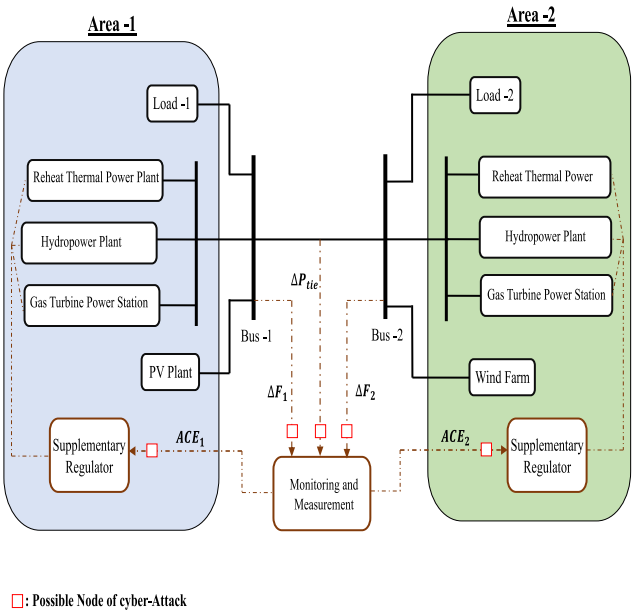

FIGURE 2. Structure of two-area interconnected power system of study with renewables.

III. PROPOSED CONTROLLER DESIGN AND METHODOLOGY

The main target of this work is to design a fractional order model reference adaptive controller (MRAC) that regulates the power input to the governor. The main advantage of the adaptive controller is its ability of adaptation with the changes

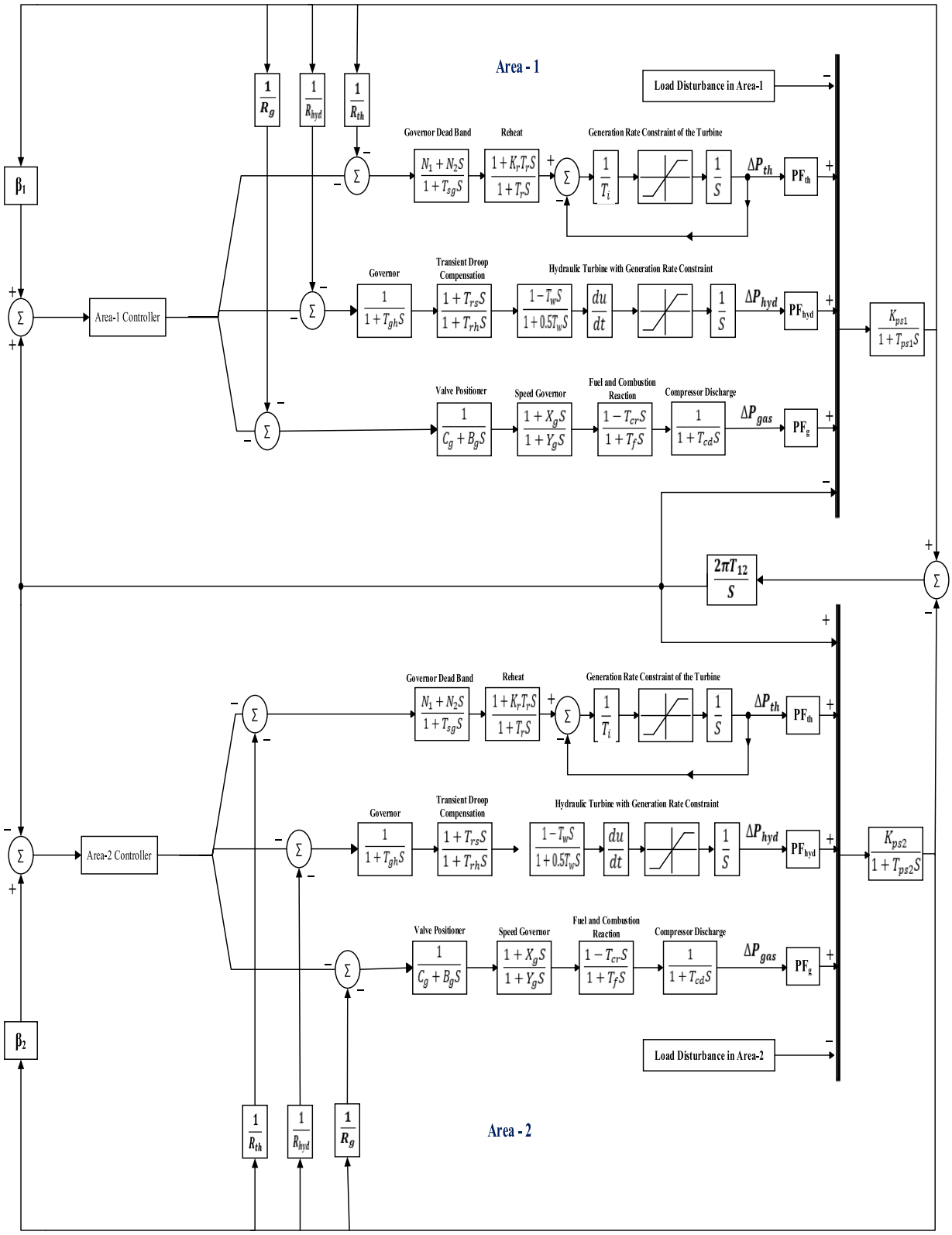

FIGURE 3. Two-area power system under study.

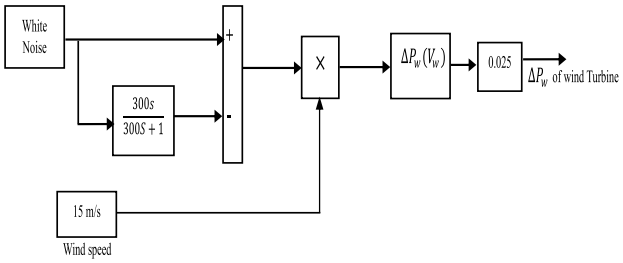

FIGURE 4. Wind power model for LFC.

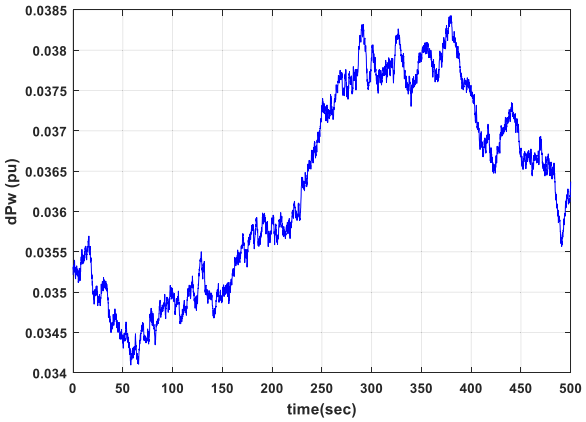

FIGURE 5. Output profile of the studied wind farm.

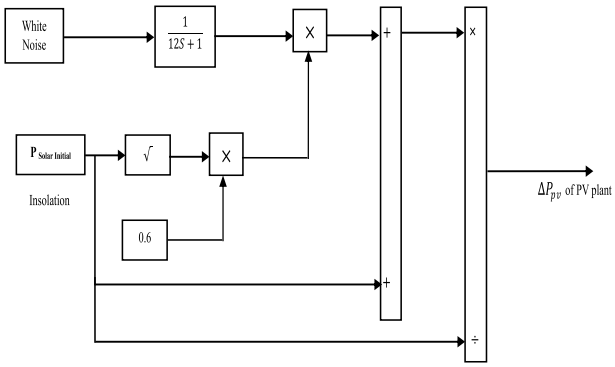

FIGURE 6. PV plant model for LFC.

in the controlled system's dynamics and disturbances according to the difference between the system output and desired output especially in case of uncertain system parameters or parameters change [40]. One of the most important schemes of MRAC is the output feedback where the only information needed from the system is the output measurement [42]. An accurate model reference needed to be tracked by the controlled system, should be properly selected. The main aim of the adaptive controller for all $t > t_0$ is to adjust the controller parameters in order to minimize the tracking error $e(t) = y(t) - y_m(t)$ so that $e(t) = 0$. $\lim_{t\to\infty}$ Where $y(t)$ is the actual plant output and $y_m(t)$ is the reference model output.

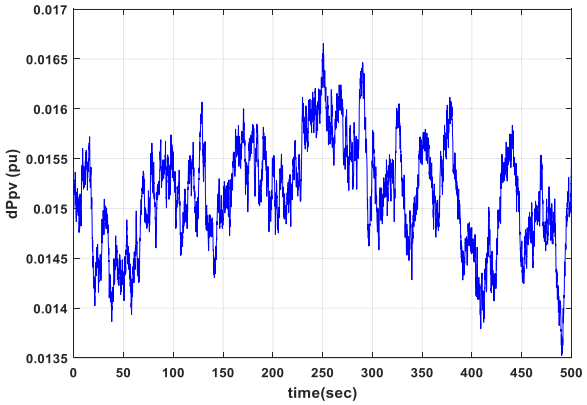

FIGURE 7. Output profile of the studied PV plant.

In order to improve the performance of the controller against the uncertainties and the unmolded dynamics, a robust adaptive modification will be adopted and combined with a disturbance observer (DO) for active disturbance rejection (ADR). The adjustment of the adaptive controller's parameters is accomplished via the integer differential equation of the adaptive low. In order to increase the robustness of the controller, the parameters adjustment can be carried out based on the fractional order differential equation of the adaptive low. The general layout of the nominated controller is illustrated in Fig. 8.

A. SUPPLEMENTARY ADAPTIVE CONTROLLER DESIGN

The design of an adaptive controller for the area control is founded on Lyapunov stability theorem in [42] and [55]. Lyapunov stability states that, provided there is a function $\boldsymbol{V} : \boldsymbol{R^n} \rightarrow \boldsymbol{R}$ that is a positive definite function such that its derivative along the trajectory solution of $\dot{x} = \boldsymbol{f(x)}$, $\frac{\boldsymbol{dV}}{\boldsymbol{dt}} = \frac{\boldsymbol{\partial V^T}}{\boldsymbol{\partial x}}\boldsymbol{f(x)}$, is a negative semidefinite then, the solution $\boldsymbol{x(t)} = 0$ to $\dot{x} = \boldsymbol{f(x)}$ is stable. Also, if $\frac{\boldsymbol{dV}}{\boldsymbol{dt}}$ is negative definite then, the solution is asymptotic stable. Moreover, if $\frac{\boldsymbol{dV}}{\boldsymbol{dt}} < 0$ and $\lim_{\|x\|\to\infty} \boldsymbol{V(x)} = \infty$ then, the solution is globally asymptotic stable. $\boldsymbol{V(x,t)}$ is called Lyapunov candidate. The stability study of Lyapunov fractional adaptive control can also be reviewed from [56] and [57]. The controller design depends on finding a Lyapunov candidate for the dynamic system so that the control signal leads the system to zero tracking error.

Assume the plant to be controlled is minimum phase system and has arbitrary transfer function (G_p) in (8). The transfer function of the reference model (G_m) in (8) should have a relative degree less than or equal to the relative degree of the controlled plant [42]. Also, the selected reference model should be strictly positive real. In the proposed controller approach, the only measured state is the system output so, auxiliary signal generators should be formed according to scheme in Fig. 9.

$$G_p(s) = K_p \frac{Z_p(s)}{R_p(s)}, \quad G_m(s) = K_m \frac{Z_m(s)}{R_m(s)}. \tag{8}$$

K_p and K_m are the natural gains of the plant and the selected reference model respectively. Assuming that, the degree of the plant is n, the degree of the auxiliary signal generators (ASG-1 and ASG-2) should equal $n-1$ [42]. Auxiliary signal generators should be built such that the reference model zeros are contained in the poles of the auxiliary generators. MRAC controller creates a control signal such that the plant output tracks the reference model output with zero tracking error. This control signal could be constructed as in (9) where $\boldsymbol{\omega}_1$ and $\boldsymbol{\omega}_2$ are the states vectors of the first and the second auxiliary signal generators respectively.

$$u_a = kr + \boldsymbol{\theta}_1^T \boldsymbol{\omega}_1 + \boldsymbol{\theta}_2^T \boldsymbol{\omega}_2 + \theta_0 y, \boldsymbol{\omega}_1, \quad \boldsymbol{\omega}_2, \boldsymbol{\theta}_1, \boldsymbol{\theta}_2 \in \mathbb{R}^{n-1}, k, \theta_0, r, y \in \mathbb{R} \tag{9}$$

$$u_a = \boldsymbol{\theta}^T \boldsymbol{\omega}, \boldsymbol{\theta}^T = \left[k\boldsymbol{\theta}_1^T \boldsymbol{\theta}_2^T \theta_0\right], \boldsymbol{\omega}^{\mathbf{T}} = \left[r\boldsymbol{\omega}_1^T \boldsymbol{\omega}_2^T y\right]. \tag{10}$$

k, $\boldsymbol{\theta}_1$, $\boldsymbol{\theta}_2$ and θ_0 are the controller parameters, r is the setpoint and y is the plant output. The ideal controller parameters have values at which the plant output can track the reference model output with zero tracking error so that $y = y_m = G_m(s)\, r$.

$$u_a^* = \boldsymbol{\theta}^{*T} \boldsymbol{\omega} = \left[k^* \boldsymbol{\theta}_1^{*T} \boldsymbol{\theta}_2^{*T} \theta_0^*\right] \begin{bmatrix} r \\ \boldsymbol{\omega}_1 \\ \boldsymbol{\omega}_2 \\ y \end{bmatrix} \tag{11}$$

$$\boldsymbol{\theta}(t) = \boldsymbol{\theta}^* + \boldsymbol{\varphi}(t) \tag{12}$$

$$u_a = \boldsymbol{\theta}^T \boldsymbol{\omega} = \boldsymbol{\theta}^{*T} \boldsymbol{\omega} + \boldsymbol{\varphi}^{\mathbf{T}} \boldsymbol{\omega}. \tag{13}$$

u_a^* is the ideal control signal, $\boldsymbol{\theta}^*$ is the vector of ideal controller parameters, $\boldsymbol{\theta}(t)$ is the vector of actual parameters at time t and $\boldsymbol{\varphi}(t)$ is the vector of parameters errors at time t. Assume the plant to be controlled is in the state space form of (14) and the reference model is in state space form of (15).

$$\dot{\boldsymbol{x}} = A\boldsymbol{x} + Bu, y = C^T \boldsymbol{x} \tag{14}$$

$$\dot{\boldsymbol{x}}_m = A_m \boldsymbol{x_m} + B_m r, y_m = C^T \boldsymbol{x_m} \tag{15}$$

$$G_p(s) = C^T (sI - A)^{-1} B \tag{16}$$

$$G_m(s) = C^T (sI - A_m)^{-1} B_m \tag{17}$$

$$\boldsymbol{e} = \boldsymbol{x} - \boldsymbol{x}_m = \left[e_1 \dot{e}_1 \ddot{e}_1 \ldots e_1^{(n-1)}\right]^T \tag{18}$$

$$e_1 = y - y_m = y - G_m(s)\, r \tag{19}$$

$$\dot{e} = A_m \boldsymbol{e} + B_m \boldsymbol{\varphi}^{\boldsymbol{T}} \boldsymbol{\omega}. \tag{20}$$

$\boldsymbol{e}$ is the tracking error vector. Assuming the linear system in (15) is asymptotic stable so, there exist a unique symmetric positive definite matrix P for each symmetric positive definite matrix Q such that [58]:

$$A_m^T P + P A_m = -Q. \tag{21}$$

As $G_m(s)$ is strictly positive real system, according to Kalman-Yakubovich lemma [58], P matrix can be chosen so that (22) and (23) can be satisfied.

$$B_m^T P = C^T \tag{22}$$

$$B_m^T P \boldsymbol{e} = C^T \boldsymbol{e} = y - y_m = e_1. \tag{23}$$

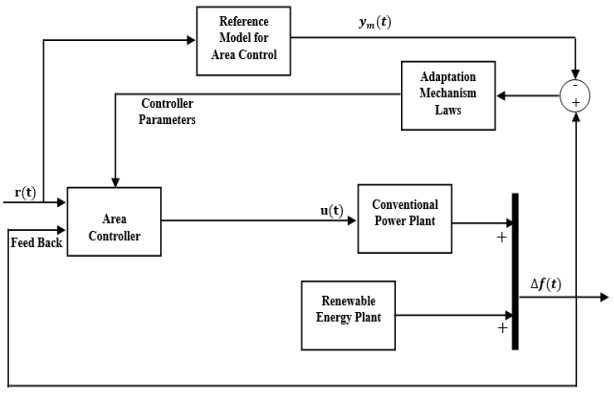

FIGURE 8. General layout design of the proposed controller.

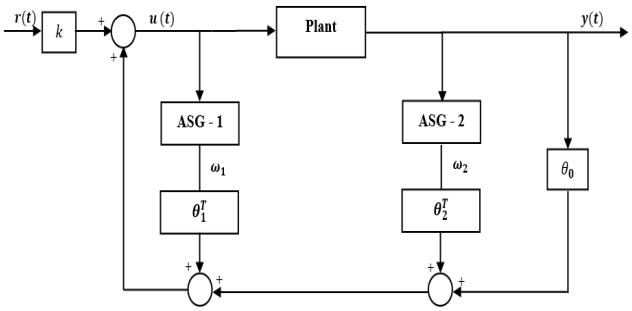

FIGURE 9. Scheme for the output feedback adaptive controller.

Lyapunov candidate function $V(e, \varphi, t)$ can be constructed to be a positive definite function of tracking error and parameters error as in (24).

$$V(\boldsymbol{e}, \boldsymbol{\varphi}, t) = \boldsymbol{e}^T P \boldsymbol{e} + \boldsymbol{\varphi}^T \Gamma^{-1} \boldsymbol{\varphi}, \Gamma > 0 \tag{24}$$

$$\dot{V}(\boldsymbol{e}, \boldsymbol{\varphi}, t) = \boldsymbol{e}^T P \dot{\boldsymbol{e}} + \dot{e}^T P \boldsymbol{e} + 2\boldsymbol{\varphi}^T \Gamma^{-1} \dot{\varphi}. \tag{25}$$

Γ is the arbitrary adaptation gain. Substitution of (20), (21) and (23) in (25) yields:

$$\dot{V}(\boldsymbol{e}, \boldsymbol{\varphi}, t) = -\boldsymbol{e}^T Q \boldsymbol{e} + 2\boldsymbol{\varphi}^T \boldsymbol{\omega} e_1 + 2\boldsymbol{\varphi}^T \Gamma^{-1} \dot{\varphi}. \tag{26}$$

In order to be sure that $\dot{V}$ is negative semidefinite and consequently, system stability can be achieved, controller parameters should be adjusted as the following:

$$\dot{\varphi} = \frac{d}{dt}\left(\boldsymbol{\theta} - \boldsymbol{\theta}^*\right) = \dot{\theta} = -\Gamma \boldsymbol{\omega} e_1. \tag{27}$$

When substituting Parameters adjustment law of (27) in (26) leads to a negative semidefinite function $\dot{V}$ as shown in (28).

$$\dot{V}(\boldsymbol{e}, \boldsymbol{\varphi}, t) = -\boldsymbol{e}^T Q \boldsymbol{e}. \tag{28}$$

The controller parameters adaptation, originally described with an integer-order derivative in (27), can be adjusted to use an arbitrary fractional-order derivative as shown in (29) [56], [57].

$${}_{t_0}^{c} D_t^{\alpha} \boldsymbol{\theta} = -\Gamma \boldsymbol{\omega} e_1, \quad 0 < \alpha \leq 1. \tag{29}$$

where ${}_{t_0}^{c}D_t^{\alpha}$ is Caputo fractional derivative operator of order α. Authors of [42] designed a modification to the adaptive low to increase robustness and to eliminate problems of parameters drift created from the high noise, uncertainties, unmodeled dynamics and nonlinearities. This modification is called e-modication which leads the controller to be robust adaptive controller with adaptive low of (30) where μ is the modification parameter.

$$ {}_{t_0}^{c}D_t^{\alpha}\boldsymbol{\theta} = -\Gamma\left(\boldsymbol{\omega} e_1 + \mu\left|e_1\right|\boldsymbol{\theta}\right). \tag{30} $$

The reference model in this study can be selected as in (31). It is shown from the Nyquist plot of G_m in Fig. 10 that, the plot lies completely in the right half side of the S-Plane which means that it is strictly positive real. Auxiliary signal generators can be selected as in (32). The symmetric positive definite P and Q matrices are designed as in (33).

$$ G_m = \frac{s^2 + 5s + 4}{s^3 + 5.2s^2 + 7s + 1.2} \tag{31} $$

$$ G_{ASG-1} = G_{ASG-2} = \frac{1}{s^2 + 5s + 4} \tag{32} $$

$$ P = \begin{bmatrix} 34 & 22 & 4 \\ 22 & 29 & 5 \\ 4 & 5 & 1 \end{bmatrix}, Q = \begin{bmatrix} 9.6 & 0 & 0 \\ 0 & 4.8 & 0 \\ 0 & 0 & 0.4 \end{bmatrix}. \tag{33} $$

B. DISTURBANCE OBSERVER DESIGN FOR ADRC

There are several disturbances, nonlinearities and dynamics that have been occurred randomly in the power system. These uncertainties can be classified into external disturbances and internal disturbances associated with the system dynamics. Due to the randomness of these disturbances, there is a persistent need to disturbances observer in order to estimate the disturbances and to eliminate them from the control signal. Accordingly, ADRC is considered as a robust control structure consisting of an observer and control signal. The process can be modelled as a general second order differential equation as follows [59]:

$$ \ddot{y} = b_0 u\left(t\right) + g\left(t, y, \dot{y}, \ldots, d, \psi\right). \tag{34} $$

where b_0 is the system gain and $g\left(.\right)$ is a function of the system output, higher dynamics, external disturbances (d) and internal disturbances and noise (ψ). As g is not measurable and considering it piecewise continuous and bounded, an estimation of it can be performed by the action of the control signal u. Let the estimators to be $\hat{x}_1 = \hat{y}$, $\hat{x}_2 = \dot{\hat{y}}$ and $\hat{x}_3 = \hat{g}$ as in general $\hat{x}$ is the estimated value of any x. The estimation lows are as follows:

$$ \dot{\hat{x}}_1\left(t\right) = \hat{x}_2\left(t\right) + l_1\left(y\left(t\right) - \hat{x}_1\left(t\right)\right) \tag{35} $$

$$ \dot{\hat{x}}_2\left(t\right) = \hat{x}_3\left(t\right) + b_0 u(t) + l_2\left(y\left(t\right) - \hat{x}_1\left(t\right)\right) \tag{36} $$

$$ \dot{\hat{x}}_3\left(t\right) = l_3\left(y\left(t\right) - \hat{x}_1\left(t\right)\right) \tag{37} $$

$$ u\left(t\right) = \frac{1}{b_0}\left(u_a\left(t\right) - \hat{g}\left(t\right)\right). \tag{38} $$

where $u_a\left(t\right)$ is the control action of the area controller that is defined in (9). Good selection of values of the observer parameters l_1, l_2 and l_3 can make the observer estimates the values of the output, dynamics and disturbances well. Tunning of the observer parameters is performed according to rules in [59].

The control low of (38) is the input to the primary control loop in Fig. 1. For applying the control low of (9) and (38) with the adaptation low of (30) on the proposed LFC control of the studied power system for each area i, signals are chosen as in (39):

$$ \boldsymbol{\omega}_i = \begin{bmatrix} ACE \\ \boldsymbol{\omega}_1 \\ \boldsymbol{\omega}_2 \\ \Delta f \end{bmatrix}_i = \begin{bmatrix} r \\ \boldsymbol{\omega}_1 \\ \boldsymbol{\omega}_2 \\ y \end{bmatrix}_i, $$

$$ u_i\left(t\right) = \left(\frac{1}{b_0}\left(u_a\left(t\right) - \hat{g}\left(t\right)\right)\right)_i = \Delta P_{ref\,i}\left(t\right). \tag{39} $$

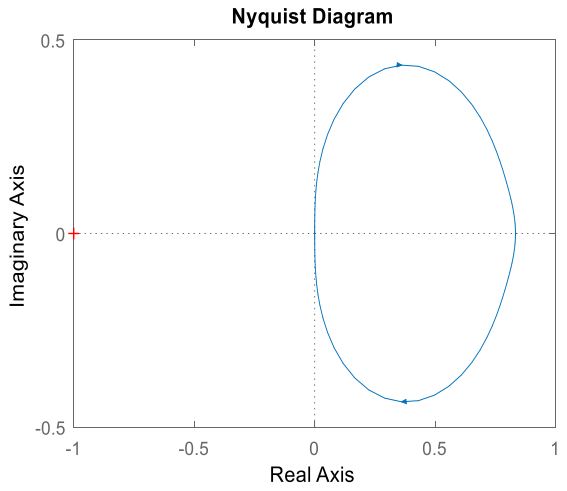

FIGURE 10. Nyquist Plot of the selected model reference of the area controller.

IV. SIMULATION AND RESULTS

The proposed controller, FOMRAC, has been implemented and tested as the main frequency controller in the double area energy system to control the frequency variations that are resulted from load perturbations. Many scenarios have been investigated to prove the outstanding performance of the proposed scheme. The proposed scheme has been compared with one of the most promising controllers that was published lately named FOPID to confirm its leading performance over that controller. For fair comparison, the parameters of the FOPID controller have been tuned using the same selected optimization algorithm named artificial rabbits optimization algorithm [48] and it is implemented on the same bases and conditions as the proposed scheme through minimizing the cost function of ITSE (Integral Time Multiplied Squared Error) shown in equation (40). The transfer function of the FOPID controller is shown in equation (41) as in [60] Where K_p, K_i and K_d are the proportional, the integral and the differential gains of the FOPID

controller respectively. The Laplace variables ($s^{-\lambda} and s^{\beta}$) has been approximated using Oustaloup approach as mentioned in [61] with a frequency band of [0.001, 1000] and with approximation order of 8. Different scenarios have been simulated as exhibited in the following subsections. This study applies its scenarios to realistic power systems as referenced in [52]. Scenario 1 and Scenario 2 address practical conditions such as load perturbations, as noted in [62]. The challenges of attenuated inertia, caused by renewable integration, a common issue in many regions [63], are simulated through scenarios involving renewable energy merging with the grid. Additionally, scenarios exploring time delay attacks and parameter changes, which can significantly impact load frequency regulation [64], are included. These simulations ensure that the study effectively represents real-world power system challenges. The simulations have been performed using MATLAB software. Furthermore, an integer-order model adaptive reference controller (IOMARC) has been carried out, and its performance has been compared to that of the fractional-order model adaptive reference controller (FOMARC) to demonstrate the superior impact of using the fractional-order regulator over the integer-order one. For more verification, another type of previously published controllers named integer order integral controller (IC) has been investigated and compared with the other three controllers at different severe conditions.

$$ITSE = \int_{t_0}^{t} t\left[\Delta f_1^2 + \Delta f_2^2 + \Delta P_{tie}^2\right]dt \tag{40}$$

$$C(s) = K_p + \frac{K_i}{s^{\lambda}} + K_d * s^{\beta}. \tag{41}$$

A. SCENARIO – 1

In this scenario, LFC controller has been used for the studied two-area system shown in Fig. 3 with no renewable energy sources. A load perturbation of 1% is applied to area-1 at 5 sec with simulation time of 300 sec. Four controllers have been implemented on the system. They are integer Integral controller (IC), FOPID controller, IOMRAC controller and the proposed FOMRAC. Artificial rabbit optimizer has been used to estimate the optimal parameters of the FOPID controllers, IC controller and the fractional orders of the FOMRAC controller. Estimated parameters of FOPID are shown in Table 2. For the robust adaptive proposed controller, a modification parameter of 0.001 has been used with different adaptation gains. For MRAC, the control action described by equation (38) has been used with adaptation gains of 10, 100, 1000 and 5000.Parameters are updated according to equation (30) with $\alpha = 1$ for both area controllers in case of integer order MRAC, while in case of fractional order MRAC, optimal values for α in (30) can be used providing extra degree of freedoms to be 0.65 and 0.75 for area-1 and 2 controllers respectively using the artificial rabbits algorithm. It should be noted that, there are increased number of oscillation cycles at high adaptation gains of 5000 for IOMRAC and that's why it is excluded as a good response has been achieved at less adaptation gain values. However, the high adaptation gain has been worked well with FOMARC and its performance has been improved due to the additional degree of freedom provided by the fractional differential adaptative equation. As demonstrated from Fig. 11, increasing the adaptive gain results in faster response towards the steady state zero deviation. It is also shown that, smaller overshoot can be achieved with smaller adaptation gain. As per NERC (North American Electric Reliability Council), the power system can withstand up to 1% overshoot of the frequency deviation with no trip and can withstand undershoot up to -2.5% for about 660 sec [49]. So as shown from this figure that, the settling time is not greater than 2.5 sec for all waves which is much less than 660 sec and the overshoot is 0.01 or less. Consequently, the high adaptation value can be used to gain the benefit of the fast response of the frequency and tie line power towards the zero deviation and the least errors as shown from Fig. 12. It is shown from the fractional order MRAC response in Fig. 13 and Fig. 14, that fast response with less errors can be achieved with the "5000" adaptation gain value that can be used without fear from losing robustness as favor of fractional adaptation. A comparison between responses and errors of the system under control of FOPID, integer IC (integer integral controller), FOMRAC (Fractional Order MRAC) and IOMRAC (Integer Order MRAC) can be shown in Fig. 15 and Fig. 16. Both IC controllers of the two areas have integral gain of 0.06 as based on the artificial rabbits optimization algorithm.

TABLE 2. Parameters of fopid controller for scenario - 1.

Area – 1	K_p	0.666
	K_i	5.4499
	K_d	2.7262
	λ	0.6092
	β	0.9905
Area – 2	K_p	0.0483
	K_i	-0.0326
	K_d	2.9286
	λ	0.1426
	β	0.9611

B. SCENARIO – 2

In this scenario, a severe customized load disturbance as shown in Fig. 17 has been implemented in area-1 to test the efficiency of the proposed FOMRAC controller compared with the other three selected controllers' IC, FOPID, IOMRAC. No renewables have been considered in the power system. The same tuned controller optimal parameters of the FOPID controller as identified in Table 2 have been used to show its response against the unexpected or unplanned disturbance action. IC controller has failed to stabilize the system against the defined load disturbance that's why, it has been excluded from the results. The adaptation gain

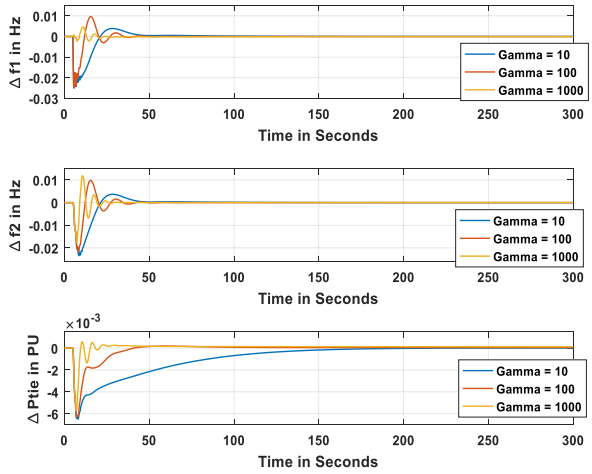

FIGURE 11. Response of integer adaptive MRAC of scenario-1.

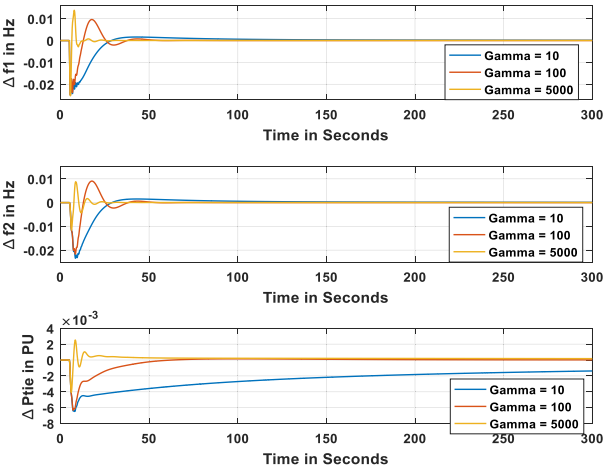

FIGURE 13. Response of fractional adaptive MRAC of scenario-1 (Order of 0.65 for area-1 and 0.75 for area-2).

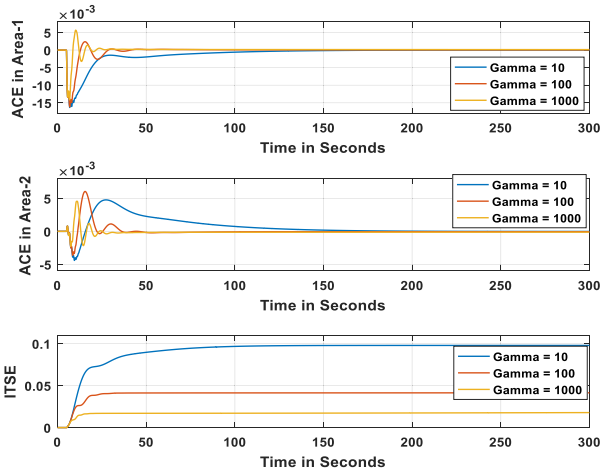

FIGURE 12. Errors response of scenario-1 Under control of the integer MRAC.

TABLE 3. Time response parameters of output waves in scenario - 2.

		FOPID	IOMRAC	FOMRAC
Maximum Overshoot	$\Delta f_1(Hz)$	0.039	0.043	0.04
	$\Delta f_2\ (Hz)$	0.035	0.048	0.035
	$\Delta P_{tie}(pu)$	0.0082	0.006	0.006
Minimum Overshoot	$\Delta f_1(Hz)$	-0.0718	-0.065	-0.064
	$\Delta f_2\ (Hz)$	-0.068	-0.061	-0.036
	$\Delta P_{tie}(pu)$	-0.012	-0.016	-0.011
	Cost Function Value	4.7976	2.1928	1.9013

parameter of the MRAC can be considered as a learning parameter. Increasing this parameter improves the tracking of the system to the reference model without any other modification of the design. However, at highly dynamics and severe environmental changes, it's essential to exercise cautions to avoid compromising stability. Conversely, to ensure safety and prevent instability caused by the parameter drift, a modification parameter (μ) would be used to enhance the adaptation as needed. Therefore, the parameters of the controller obtained from the first scenario have remained unchanged. Thus, a fractional order of 0.65 has been retained for Area-1 FOMRAC, while Area-2 FOMRAC has maintained a fractional order of 0.75. The modification parameter remains consistent at 0.001 for both FOMRAC and IOMRAC in both areas with a slight reduction in the adaptation gain. This approach has eliminated the need of reusing the optimization algorithm for MRAC within this framework and the controller's self-adaptation to various disturbance actions has been established.

As shown in Fig. 18, Fig. 19, Fig. 20 and Fig. 21, the results have been closely resembling those of the first scenario for MRAC, indicating an enhanced fast response with the increasing of the adaptation gain. Furthermore, FOMRAC has demonstrated slightly superior performance compared to IOMRAC, as it allows a greater chance of increased adaptation gain. However as shown in Fig. 22 and Fig. 23, the utilization of the FOPID controller have stabilized the system with exhibiting overshoots. Nonetheless, undershoots have been observed with the FOPID controller, and the system stabilizes at a nonzero value, resulting in a non-zero steady-state error compared to FOMRAC and IOMRAC. According to the time response parameters of the output waves of Fig. 22 and Fig. 23 that have been listed in Table 3, ITSE in the case of FOPID has been greater than that of IOMRAC and FOMRAC. Better transient response has been achieved upon using IOMRAC or FOMRAC via decreasing the adaptation gain, but the steady-state response will not be superior than that achieved with the higher adaptation gain. As illustrated in Table 3, FOMRAC shows a relative enhancement in cost function of 15% and 152% compared to IOMRAC and FOPID controllers respectively.

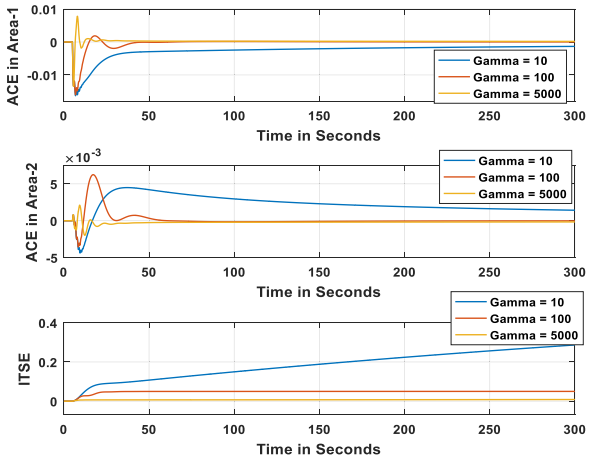

FIGURE 14. Errors of scenario-1 with control of FOMRAC (order of 0.65 for area-1 and 0.75 for area-2).

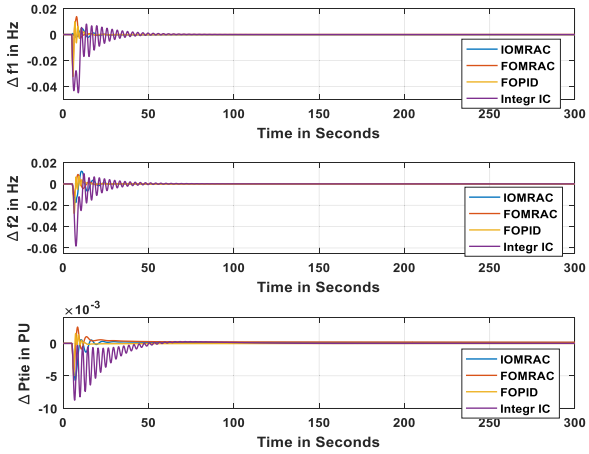

FIGURE 15. Responses of different controllers of scenario-1.

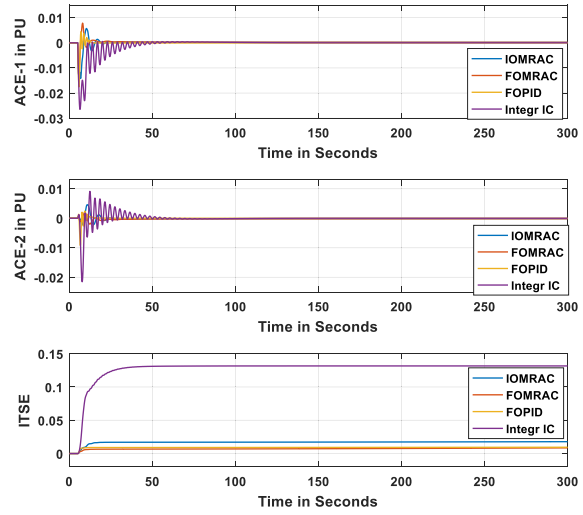

FIGURE 16. Errors of scenario-1 with different controllers.

C. SCENARIO-3

This scenario tests the performance of the two-area power system under the control of FOPID, FOMRAC and IOMRAC against a load disturbance and during insertion of renewables. A load disturbance of 1% has been emulated in area-1 at 5 sec,

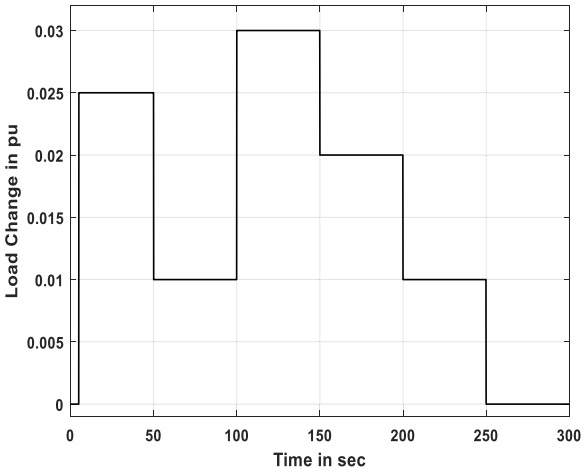

FIGURE 17. Customized load change at different instants with different values.

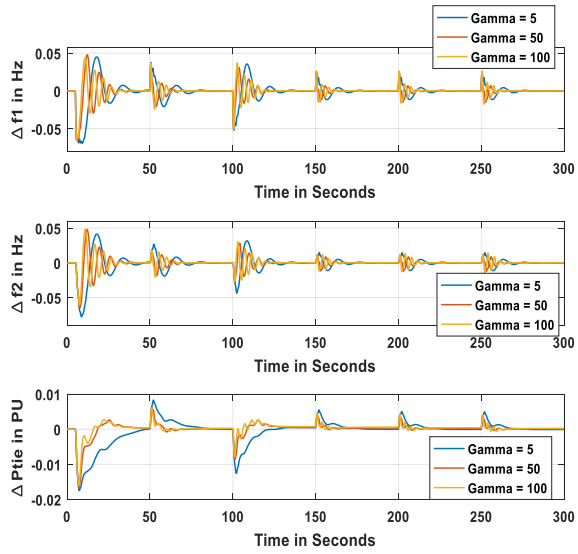

FIGURE 18. Response of integer adaptive MRAC of scenario-2.

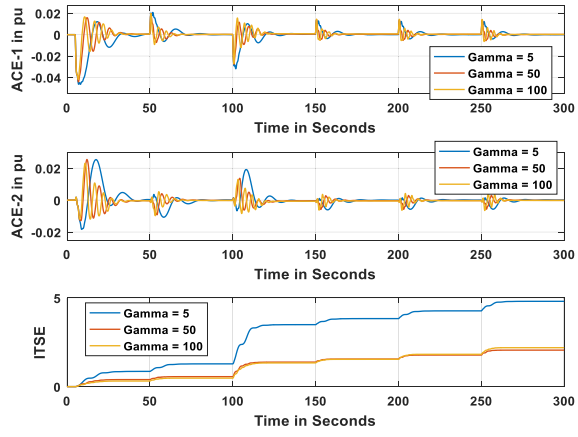

FIGURE 19. Errors response of scenario-2 under control of the integer MRAC.

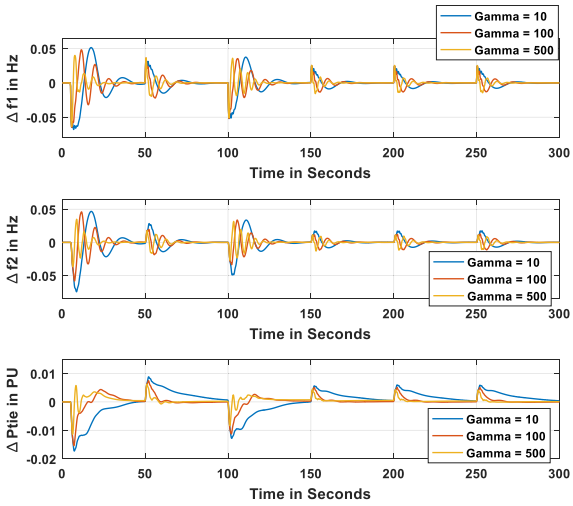

FIGURE 20. Response of FOMRAC of Scenario-2 (order of 0.65 for area- 1 and 0.75 for area-2).

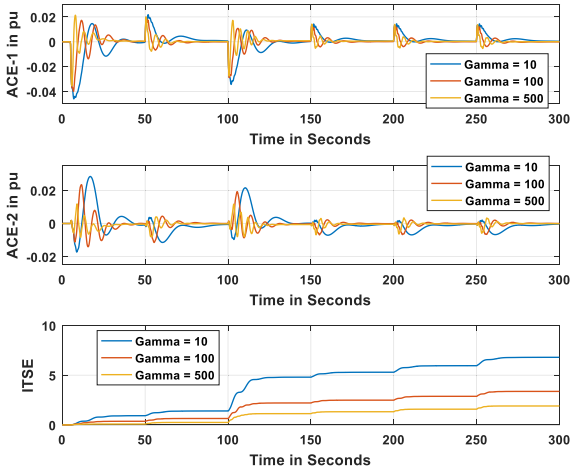

FIGURE 21. Errors of scenario-2 with control of FOMRAC (order of 0.65 for area-1 and 0.75 for area-2).

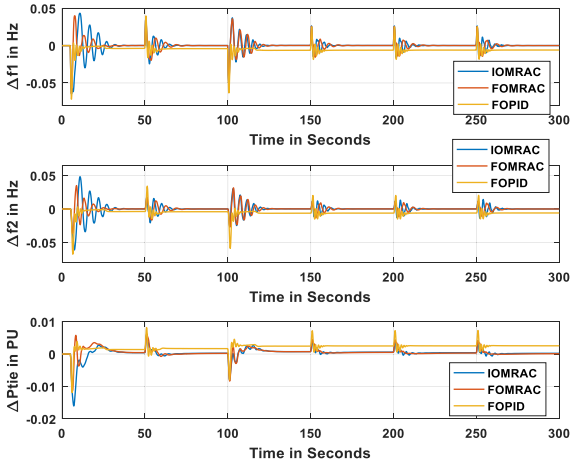

FIGURE 22. Responses of different controllers of scenario-2.

a windfarm has been connected to the area-2 at 50 sec and a PV plant has been inserted to the area-1 at 150 sec within

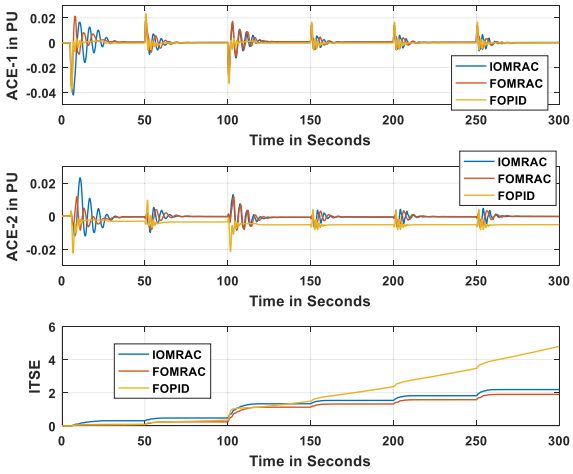

FIGURE 23. Errors of scenario-2 with different controllers.

a simulation time of 300 sec. The FOPID parameters have to be retuned optimally to match the reconfiguration of the model so, they have been listed in Table 4. While, thanks to their adaptive capability, the modification parameters of the IOMRAC and FOMRAC and the fractional orders of the FOMRAC have no need to be changed and they have been applicable as in case of scenario-1 and scenario-2. Moreover, the reference models of both MRAC controllers haven't been varied from scenario-1 or scenario-2.

The output response of the system has been stabilized under the control of the three controllers as shown from Fig. 24, Fig. 25 and Table 5. However, better transient and steady state responses have been detected in case of the FOMRAC with the lowest ITSE value, the lowest overshoot and the fastest response towards the steady state. IOMRAC has shown the highest ITSE value among the three controllers as its oscillations have damped after relatively longer time. In case of FOPID controller, a high overshoot has been occurred comparing to IMORAC and FOMRAC. It is worth noting that the FOPID controller retuning has been needed in this scenario to achieve the stability while, in case of FOMRAC and IOMRAC, there is no need for that because of their ability to adapt themselves with the new conditions without any change of the reference model, modification parameters or fractional orders. FOMRAC shows a relative enhancement in cost function of 75% and 29% compared to IOMRAC and FOPID controllers respectively.

D. SCENARIO-4

Time delay is one of the undesirable attacks that may occur to the controller and it may negatively affect the system response. This scenario emulates the behavior of the FOPID, IOMRAC and FOMRAC controllers under these time delays. Therefore, time delays of 0.01 sec and 0.1 sec have been applied to the controllers' outputs for both areas. Furthermore, a 1% load perturbation has been applied to area-1 at 5 sec and a 1% load perturbation has been applied to

TABLE 4. Parameters of FOPID controller for scenario - 3.

Area – 1	K_p	1.8204
	K_i	0.7157
	K_d	1.8087
	λ	0.6661
	β	0.9434
Area – 2	K_p	1.0516
	K_i	2.5899
	K_d	3.4995
	λ	0.95
	β	0.95

TABLE 5. Some time response parameters of output waves in scenario – 3.

		FOPID	IOMRAC	FOMRAC
Maximum Overshoot	$\Delta f_1(Hz)$	0.088	0.061	0.048
	$\Delta f_2\ (Hz)$	0.084	0.081	0.081
	$\Delta P_{tie}(pu)$	0.008	0.006	0.006
Minimum Overshoot	$\Delta f_1(Hz)$	-0.036	-0.055	-0.04
	$\Delta f_2\ (Hz)$	-0.049	-0.049	-0.05
	$\Delta P_{tie}(pu)$	-0.015	-0.017	-0.014
	Cost Function Value	2.0418	2.7786	1.5864

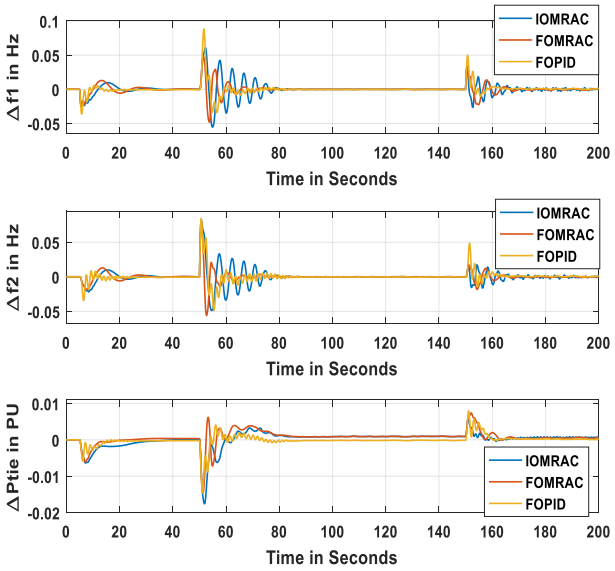

FIGURE 24. Responses of different controllers of scenario-3.

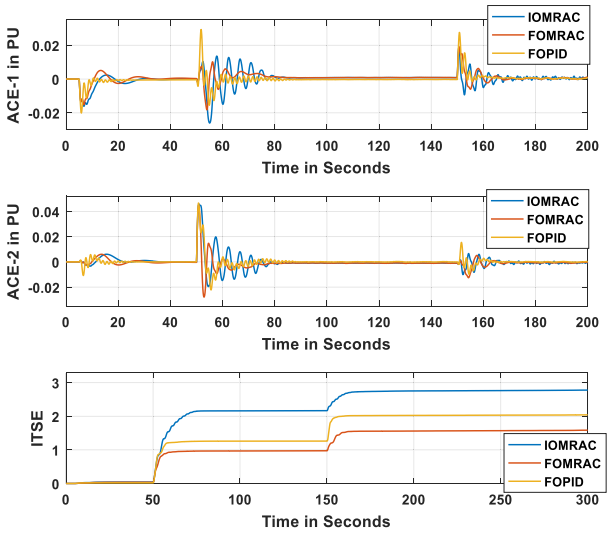

FIGURE 25. Errors of scenario-3 with different controllers.

TABLE 6. Some time response parameters of output waves in scenario – 4 with 0.01 SEC delay time.

		FOPID	IOMRAC	FOMRAC
Maximum Overshoot	$\Delta f_1(Hz)$	0.092	0.069	0.048
	$\Delta f_2\ (Hz)$	0.087	0.082	0.081
	$\Delta P_{tie}(pu)$	0.008	0.006	0.006
Minimum Overshoot	$\Delta f_1(Hz)$	-0.037	-0.059	-0.04
	$\Delta f_2\ (Hz)$	-0.052	-0.054	-0.06
	$\Delta P_{tie}(pu)$	-0.015	-0.019	-0.014
	Cost Function Value	2.9272	3.3244	1.8532

TABLE 7. Some time response parameters of output waves in scenario – 4 with 0.1 SEC delay time.

		FOPID	IOMRAC	FOMRAC
Maximum Overshoot	$\Delta f_1(Hz)$	0.053	0.09	0.08
	$\Delta f_2\ (Hz)$	0.072	0.09	0.08
	$\Delta P_{tie}(pu)$	0.006	0.007	0.0059
Minimum Overshoot	$\Delta f_1(Hz)$	-0.075	-0.076	-0.078
	$\Delta f_2\ (Hz)$	-0.079	-0.076	-0.07
	$\Delta P_{tie}(pu)$	-0.014	-0.02	-0.019
	Cost Function Value	76.6	13.1	12.3

area-2 at 180 sec with simulation time of 300 sec. Parameters of FOPID controller have the same values as listed in Table 4.

It is shown from Fig. 26, Fig. 27 and Table 6 that in case of 0.01 sec time delay, all controllers can stabilize the system. However, the maximum overshoot of FOPID controller is higher than that of IOMRAC and FOMRAC. FOMRAC has shown a dominant behavior with less oscillations, fastest response towards the zero steady state and less ITSE error compared to FOPID and IOMRAC. However, in case of 0.1 sec time delay as shown in Fig. 28, the FOPID controller has displayed undamped oscillations within ±4.5%. While, both of IOMRAC and FOMRAC can stabilize the system with undamped oscillations within ±1% that is within the allowable limit of NREC. Moreover, in case of 0.1 sec, FOPID

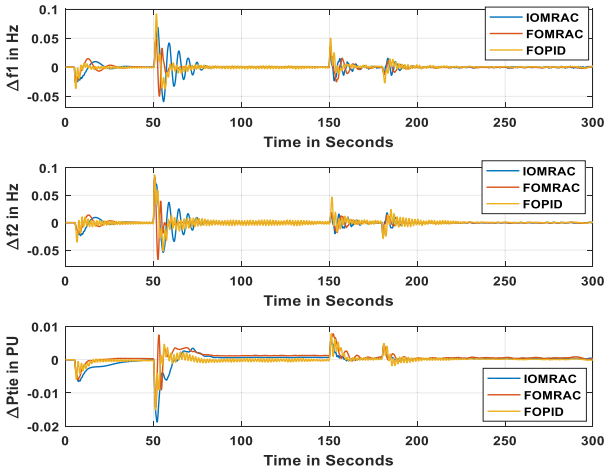

FIGURE 26. Response of different controllers with 0.01 sec time delay in scenario-4.

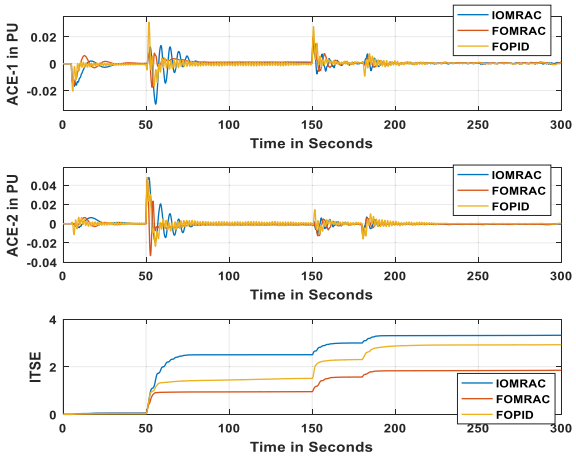

FIGURE 27. Errors with different controllers in scneario-4 with 0.01 sec time delay.

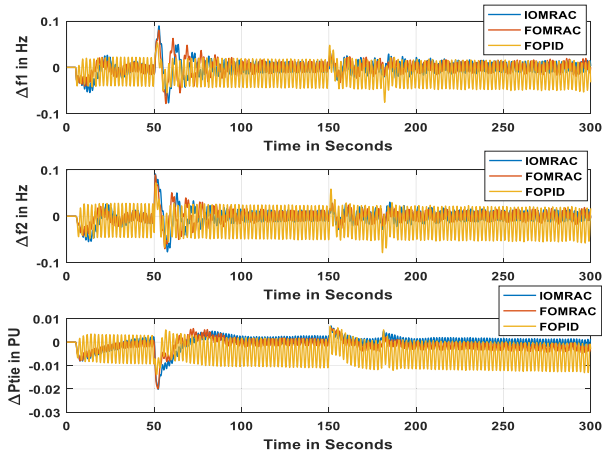

FIGURE 28. Response of different controllers with 0.1 sec time delay in scenario-4.

has presented very high increasing and unsteady ITSE error value compared to IOMRAC and FOMRAC as shown from

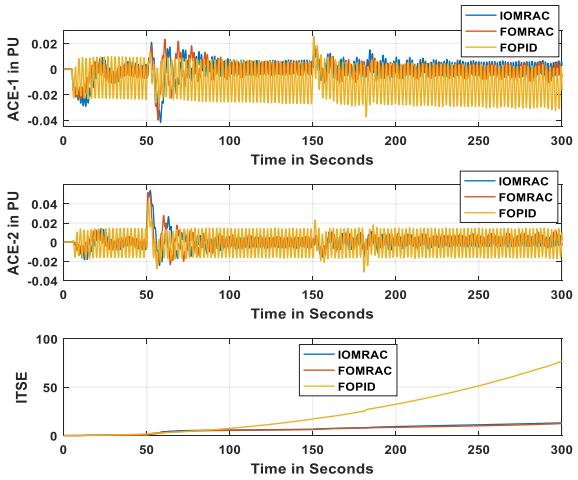

FIGURE 29. Errors with different controllers in scneario-4 with 0.1 sec time delay.

TABLE 8. Some time response parameters of output waves in scenario - 5.

Change Percentage		+50%		−50%	
Controller		FOPID	FOMRAC	FOPID	FOMRAC
Area-1	$\Delta f_1(Hz)$	0.09	0.048	0.085	0.042
	$\Delta f_2\ (Hz)$	0.085	0.08	0.087	0.072
	$\Delta P_{tie}(pu)$	0.09	0.009	0.011	0.007
Area-2	$\Delta f_1(Hz)$	-0.067	-0.049	-0.074	-0.048
	$\Delta f_2\ (Hz)$	-0.062	-0.058	-0.073	-0.041
	$\Delta P_{tie}(pu)$	-0.0144	-0.015	-0.014	-0.012
Cost Function Value		5.56	4.21	13.71	6.91

Fig. 29 and Table 7. This scenario has shown a very strong aspect of using the proposed FOMRAC controller which is its ability to adapt itself against any different situations that may occur during the operation and therefore it is recommended to be used in achieving a continuous online tuning during any change in the system conditions. In case of 0.01 sec delay time, cost function relative enhancement of 79% and 58% can be shown by the FOMRAC when compared to IOMRAC and FOPID respectively. While in case of 0.1 sec delay, cost function relative enhancement of 6.5% and 522% can be shown by the FOMRAC when compared to IOMRAC and FOPID respectively.

E. SCENARIO-5

In this scenario, the performance of FOPID and FOMRAC is tested against ±50% change in system parameters with the insertion of RESs. This parameter change action has been adopted for T_{sg} and T_{rh} parameters in the second area of Fig. 3. The PV station has been linked to the first area at 150 sec and the wind farm has been connected to the area-2 at 50 sec. Furthermore, a demand perturbation of 2% has been implemented in the first area at 100 sec and a

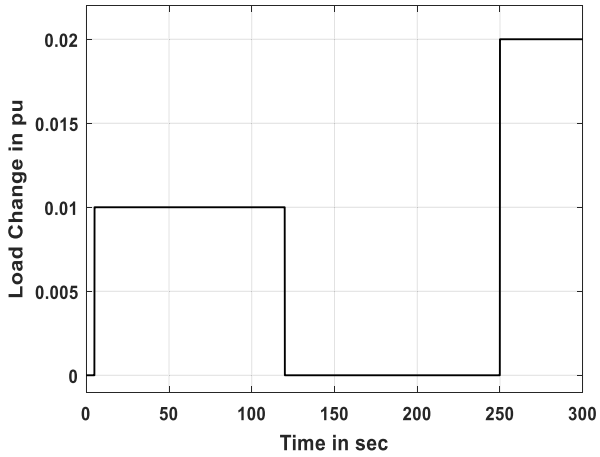

FIGURE 30. A customized load disturbance applied to area-2 for scenario-5.

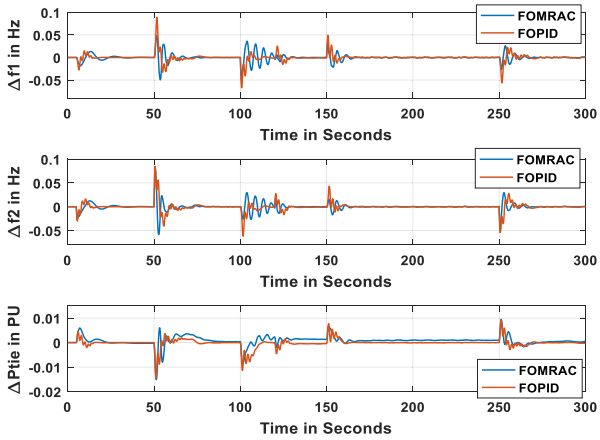

FIGURE 31. System response under effect of different controllers after +50% parameters change.

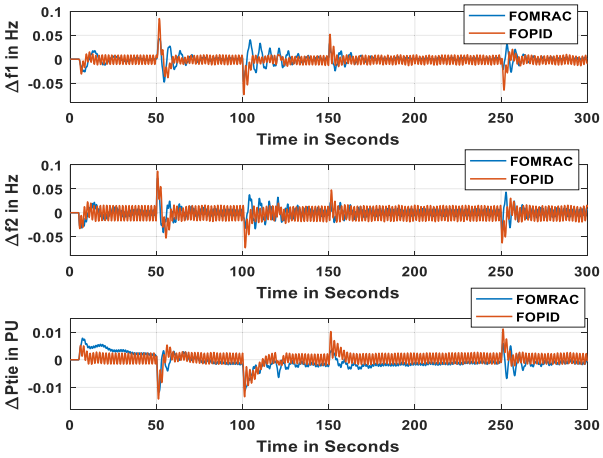

FIGURE 32. System response under effect of different controllers after -50% parameters change.

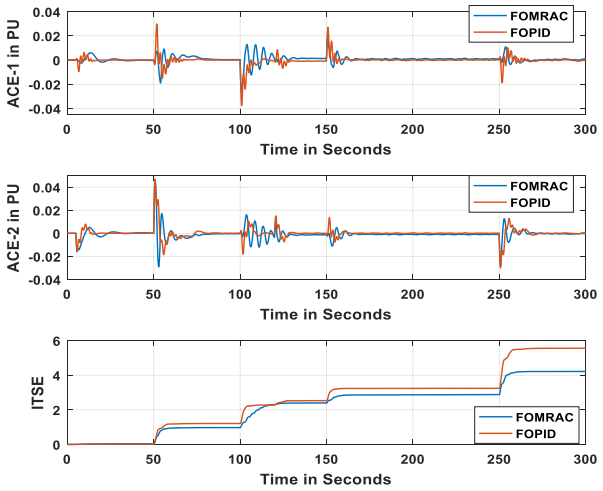

FIGURE 33. System errors under effect of different controllers after +50% parameters change.

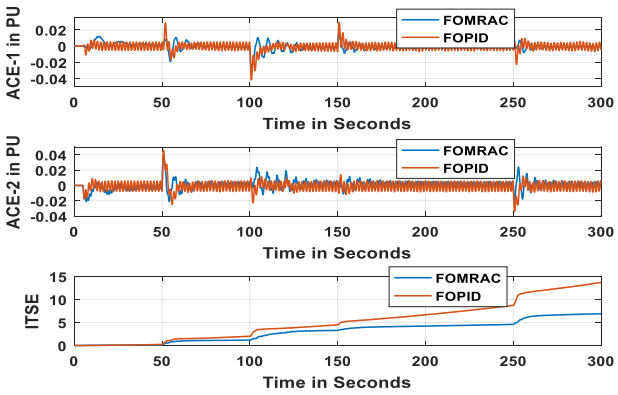

FIGURE 34. System errors under effect of different controllers after -50% parameters change.

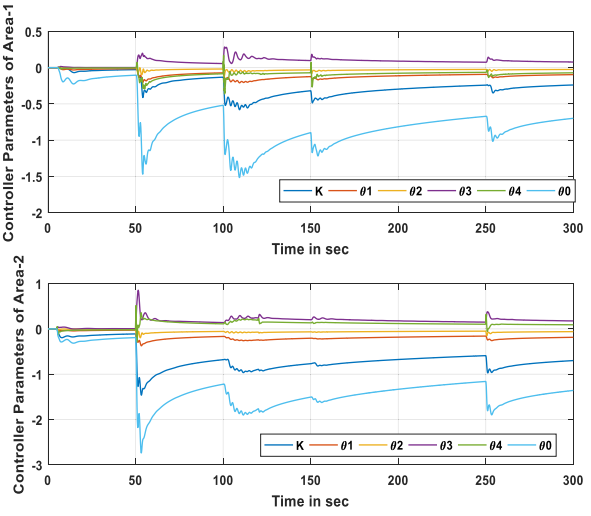

FIGURE 35. Proposed FOMRAC Parameters during +50% change in power system parameters.

customized demand perturbation of Fig. 30 has been applied to area-2. A simulation time of 300 sec has been accomplished. The same parameters of FOPID controller as in Table 4 have been used in this scenario. According to Fig. 31, Fig. 32 and Table 8, FOMRAC is able to tackle with the parameters change better than the FOPID controller. Errors

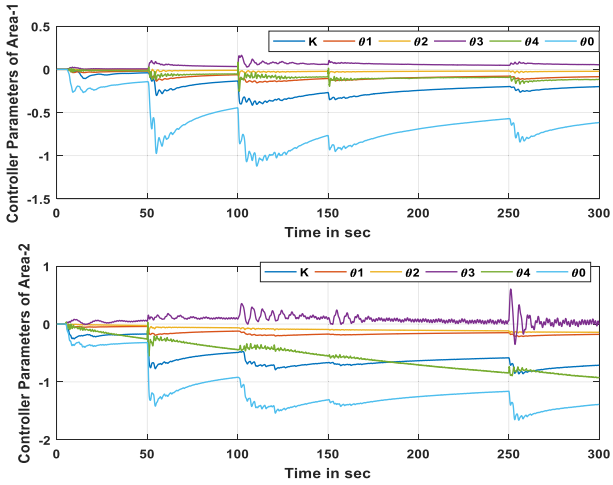

FIGURE 36. Proposed FOMRAC parameters during -50% change in power system parameters.

in the case of FOMRAC have been lower than that of FOPID controllers as shown in Fig. 33 and Fig. 34. Maximum overshoots have increased in the case of FOPID controllers to values higher than that of FOMRAC. FOMRAC shows an enhancement in the cost function of 32% against the FOPID controller in case of +50% change in system parameters and 98% enhancement in case of −50% change in system parameters. That's why the proposed control methodology has been recommended for real time control of the load frequency thanks to its ability to adapt itself during sever changes in the system parameters.

The main purpose of this scenario is to check the robustness and the sensitivity of the proposed controller against the system parameters changes which are frequent in current complex systems. A major advantage of the proposed FOMRAC is its ability to adapt itself and adjust its parameters by itself online and continuously against the changes in the system parameters. Fig. 31 and Fig. 32 shows the robustness of the proposed FOMRAC. Furthermore Fig. 35 and Fig. 36 show the self-adjustment of the proposed controller parameters ($\boldsymbol{\theta}^T$ of (10)) to overcome the situation of ±50% system parameters change.

V. CONCLUSION

Secondary area dynamic control for load frequency regulation in the two-area hybrid conventional & renewable power system to provide perfect response adaptively is the main target of this work. It is well known that, the renewables negatively affect the performance of load frequency controllers as a result of the decreased system inertia resulting from the higher number of semiconducting devices and static generators so, a robust adaptive control scheme would be good option to control the system frequency in multi area power system with and without renewables. That's why, a novel real time adaptive control scheme that includes FOMRAC and a disturbance rejection observer has been proposed as an efficient closed loop load frequency controller that is able to dynamically adjust its parameters online by itself which is a key advantage of the FOMRAC controller that it is its adaptive capability, relying solely on system output for different tested cases without need to alter its main parameters, resulting in minimal ITSE error compared to other controllers. The proposed scheme has been tested during severe load variations and while considering system parameters disturbances. Moreover, its behavior has been investigated during time delay attacks. For more verification of the proposed scheme, its results have been compared to that of the most recent previously published schemes to prove its efficiency and robustness over the others. In all scenarios, results show that enhancement in cost function is ranging from 29% to 522% when using the proposed FOMRAC as compared to FOPID controller while the enhancement in cost function when using the proposed FOMRAC controller ranges from 15% to 80% when compared to the IOMRAC. Therefore, the proposed controller is highly recommended to be applied for frequency regulation in multi area hybrid power systems.

REFERENCES

[1] P. Kundur, "Definition and classification of power system stability IEEE/CIGRE joint task force on stability terms and definitions," *IEEE Trans. Power Syst.*, vol. 19, no. 3, pp. 1387–1401, Aug. 2004.
[2] C. T. Force, "Large frequency disturbances: Analysis and modeling needs," in *Proc. IEEE Power Eng. Soc. Winter Meeting*, vol. 1, New York, NY, USA, Jan. 1999, pp. 554–558.
[3] R. Shankar and P. Kundur, *Power System Stability and Control II*. New York, NY, USA: McGraw-Hill, 1994.
[4] W. Zhang and K. Fang, "Controlling active power of wind farms to participate in load frequency control of power systems," *IET Gener., Transmiss. Distrib.*, vol. 11, no. 9, pp. 2194–2203, Jun. 2017.
[5] L. Fan, *Control and Dynamics in Power Systems and Microgrids*. Boca Raton, FL, USA: CRC Press, 2017.
[6] H. Abubakr, J. C. Vasquez, T. Hassan Mohamed, and J. M. Guerrero, "The concept of direct adaptive control for improving voltage and frequency regulation loops in several power system applications," *Int. J. Electr. Power Energy Syst.*, vol. 140, Sep. 2022, Art. no. 108068.
[7] A. Kumar and M. N. Anwar, "Decentralized load–frequency controller design for a single as well as multi-area power system," *Iranian J. Sci. Technol., Trans. Electr. Eng.*, vol. 44, no. 1, pp. 309–326, Mar. 2020.
[8] D. G. Padhan and S. Majhi, "A new control scheme for PID load frequency controller of single-area and multi-area power systems," *ISA Trans.*, vol. 52, no. 2, pp. 242–251, Mar. 2013.
[9] V. P. Singh, N. Kishor, and P. Samuel, "Distributed multi-agent system-based load frequency control for multi-area power system in smart grid," *IEEE Trans. Ind. Electron.*, vol. 64, no. 6, pp. 5151–5160, Jun. 2017.
[10] N. E. L. Y. Kouba, M. Menaa, M. Hasni, and M. Boudour, "Load frequency control in multi-area power system based on fuzzy logic-PID controller," in *Proc. IEEE Int. Conf. Smart Energy Grid Eng. (SEGE)*, Aug. 2015, pp. 1–6.
[11] S. Prasad, S. Purwar, and N. Kishor, "Non-linear sliding mode load frequency control in multi-area power system," *Control Eng. Pract.*, vol. 61, pp. 81–92, Apr. 2017.
[12] Y. P. Verma and A. Kumar, "Load frequency control in deregulated power system with wind integrated system using fuzzy controller," *Frontiers Energy*, vol. 7, no. 2, pp. 245–254, Jun. 2013.
[13] W. Tan, H. Zhang, and M. Yu, "Decentralized load frequency control in deregulated environments," *Int. J. Electr. Power Energy Syst.*, vol. 41, no. 1, pp. 16–26, Oct. 2012.
[14] K. Chatterjee, "Design of dual mode PI controller for load frequency control," *Int. J. Emerg. Electr. Power Syst.*, vol. 11, no. 4, pp. 60–85, Sep. 2010.
[15] L. C. Saikia, J. Nanda, and S. Mishra, "Performance comparison of several classical controllers in AGC for multi-area interconnected thermal system," *Int. J. Electr. Power Energy Syst.*, vol. 33, no. 3, pp. 394–401, Mar. 2011.

[16] N. C. Patel, M. K. Debnath, D. P. Bagarty, and P. Das, "Load frequency control of a non-linear power system with optimal PID controller with derivative filter," in *Proc. IEEE Int. Conf. Power, Control, Signals Instrum. Eng. (ICPCSI)*, Sep. 2017, pp. 1515–1520.

[17] J. Yang, Q. Zhong, A. M. Y. M. Ghias, Z. Y. Dong, K. Shi, and Y. Yu, "Distributed fault-tolerant PI load frequency control for power system under stochastic event-triggered scheme," *Appl. Energy*, vol. 351, Dec. 2023, Art. no. 121844.

[18] L. Wang, *Model Predictive Control System Design and Implementation Using MATLAB*. Cham, Switzerland: Springer, 2009.

[19] M. Elsisi, M. Soliman, M. A. S. Aboelela, and W. Mansour, "Bat inspired algorithm based optimal design of model predictive load frequency control," *Int. J. Electr. Power Energy Syst.*, vol. 83, pp. 426–433, Dec. 2016.

[20] Y. Zheng, J. Zhou, Y. Xu, Y. Zhang, and Z. Qian, "A distributed model predictive control based load frequency control scheme for multi-area interconnected power system using discrete-time Laguerre functions," *ISA Trans.*, vol. 68, pp. 127–140, May 2017.

[21] A. M. Kassem, "Neural predictive controller of a two-area load frequency control for interconnected power system," *Ain Shams Eng. J.*, vol. 1, no. 1, pp. 49–58, Sep. 2010.

[22] J. Liu, Q. Yao, and Y. Hu, "Model predictive control for load frequency of hybrid power system with wind power and thermal power," *Energy*, vol. 172, pp. 555–565, Apr. 2019.

[23] S. H. Shahalami and D. Farsi, "Analysis of load frequency control in a restructured multi-area power system with the Kalman filter and the LQR controller," *AEU Int. J. Electron. Commun.*, vol. 86, pp. 25–46, Mar. 2018.

[24] E. E. Vlahakis, L. D. Dritsas, and G. D. Halikias, "Distributed LQR design for identical dynamically coupled systems: Application to load frequency control of multi-area power grid," in *Proc. IEEE 58th Conf. Decis. Control (CDC)*, Dec. 2019, pp. 4471–4476.

[25] W.-H. Chen, J. Yang, L. Guo, and S. Li, "Disturbance-observer-based control and related methods—An overview," *IEEE Trans. Ind. Electron.*, vol. 63, no. 2, pp. 1083–1095, Feb. 2016.

[26] D. Guha, P. K. Roy, and S. Banerjee, "Disturbance observer aided optimised fractional-order three-degree-of-freedom tilt-integral-derivative controller for load frequency control of power systems," *IET Gener., Transmiss. Distrib.*, vol. 15, no. 4, pp. 716–736, Feb. 2021.

[27] C. Chen, K. Zhang, K. Yuan, Z. Gao, X. Teng, and Q. Ding, "Disturbance rejection-based LFC for multi-area parallel interconnected AC/DC system," *IET Gener., Transmiss. Distrib.*, vol. 10, no. 16, pp. 4105–4117, Dec. 2016.

[28] C. Wang, Y. Mi, Y. Fu, and P. Wang, "Frequency control of an isolated micro-grid using double sliding mode controllers and disturbance observer," *IEEE Trans. Smart Grid*, vol. 9, no. 2, pp. 923–930, Mar. 2018.

[29] I. Petráš, "Tuning and implementation methods for fractional-order controllers," *Fractional Calculus Appl. Anal.*, vol. 15, no. 2, pp. 282–303, Jun. 2012.

[30] S. Sondhi and Y. V. Hote, "Fractional order PID controller for load frequency control," *Energy Convers. Manage.*, vol. 85, pp. 343–353, Sep. 2014.

[31] S. Sondhi and Y. V. Hote, "Fractional order PID controller for perturbed load frequency control using Kharitonov's theorem," *Int. J. Electr. Power Energy Syst.*, vol. 78, pp. 884–896, Jun. 2016.

[32] S. Saxena, "Load frequency control strategy via fractional-order controller and reduced-order modeling," *Int. J. Electr. Power Energy Syst.*, vol. 104, pp. 603–614, Jan. 2019.

[33] A. Elmelegi, E. A. Mohamed, M. Aly, E. M. Ahmed, A. A. Mohamed, and O. Elbaksawi, "Optimized tilt fractional order cooperative controllers for preserving frequency stability in renewable energy-based power systems," *IEEE Access*, vol. 9, pp. 8261–8277, 2021.

[34] E. A. Mohamed, E. M. Ahmed, A. Elmelegi, M. Aly, O. Elbaksawi, and A. A. Mohamed, "An optimized hybrid fractional order controller for frequency regulation in multi-area power systems," *IEEE Access*, vol. 8, pp. 213899–213915, 2020.

[35] S. V. Sah, V. Prakash, P. K. Pathak, and A. K. Yadav, "Fractional order AGC design for power systems via artificial gorilla troops optimizer," in *Proc. IEEE Int. Conf. Power Electron., Drives Energy Syst. (PEDES)*, Jaipur, India, Dec. 2022, pp. 1–6.

[36] H. A. Yousef, K. AL-Kharusi, M. H. Albadi, and N. Hosseinzadeh, "Load frequency control of a multi-area power system: An adaptive fuzzy logic approach," *IEEE Trans. Power Syst.*, vol. 29, no. 4, pp. 1822–1830, Jul. 2014.

[37] C. M. Liaw, "Design of a reduced-order adaptive load-frequency controller for an interconnected hydrothermal power system," *Int. J. Control*, vol. 60, no. 6, pp. 1051–1063, Dec. 1994.

[38] A. Rubaai, "Self-tuning load frequency control: Multilevel adaptive approach," *IEE Proc. Gener., Transmiss. Distrib.*, vol. 141, no. 4, p. 285, 1994.

[39] S. Nema, V. Prakash, and H. Pandžic, "Adaptive synthetic inertia control framework for distributed energy resources in low-inertia microgrid," *IEEE Access*, vol. 10, pp. 54969–54979, 2022.

[40] G. Tao, *Adaptive Control Design and Analysis*, vol. 37. Hoboken, NJ, USA: Wiley, 2003.

[41] H. Kaufman, I. Barkana, and K. Sobel, *Direct Adaptive Control Algorithms: Theory and Applications*. Cham, Switzerland: Springer, 2012.

[42] K. S. Narendra and A. M. Annaswamy, *Stable Adaptive Systems*. Chelmsford, MA, USA: Courier Corporation, 2012.

[43] N. Hovakimyan, C. Cao, E. Kharisov, E. Xargay, and I. M. Gregory, "L1 adaptive control for safety-critical systems," *IEEE Control Syst. Mag.*, vol. 31, no. 5, pp. 54–104, Oct. 2011.

[44] B. M. Vinagre, I. Petráš, I. Podlubny, and Y. Q. Chen, "Using fractional order adjustment rules and fractional order reference models in model-reference adaptive control," *Nonlinear Dyn.*, vol. 29, pp. 269–279, Jul. 2002.

[45] C. T. Pan and C. M. Liaw, "An adaptive controller for power system load-frequency control," *IEEE Power Eng. Rev.*, vol. 9, no. 2, pp. 45–46, Jan. 1989.

[46] F. Sattar, S. Ghosh, Y. J. Isbeih, M. S. El Moursi, A. Al Durra, and T. H. M. El Fouly, "A predictive tool for power system operators to ensure frequency stability for power grids with renewable energy integration," *Appl. Energy*, vol. 353, Jan. 2024, Art. no. 122226.

[47] A. Ragab, D. Allam, and H. A. Attia, "Supporting load frequency control process by using adaptive model reference virtual inertia controller when connecting renewable energy plants," *Comput. Electr. Eng.*, vol. 117, Jul. 2024, Art. no. 109295.

[48] L. Wang, Q. Cao, Z. Zhang, S. Mirjalili, and W. Zhao, "Artificial rabbits optimization: A new bio-inspired meta-heuristic algorithm for solving engineering optimization problems," *Eng. Appl. Artif. Intell.*, vol. 114, Sep. 2022, Art. no. 105082.

[49] H. Bevrani, *Robust Power System Frequency Control*, vol. 4. Cham, Switzerland: Springer, 2014.

[50] H. Shayeghi, H. A. Shayanfar, and A. Jalili, "Load frequency control strategies: A state-of-the-art survey for the researcher," *Energy Convers. Manage.*, vol. 50, no. 2, pp. 344–353, Feb. 2009.

[51] S. Saxena, S. Bhatia, and R. Gupta, "Cybersecurity analysis of load frequency control in power systems: A survey," *Designs*, vol. 5, no. 3, p. 52, Aug. 2021.

[52] C. S. Rao, "Improvement of dynamic performance of AGC of hydrothermal system employing capacitive energy storage and TCPS," *Innov. Syst. Des. Eng.*, vol. 2, no. 6, pp. 63–71, Oct. 2011.

[53] T. Michigami and T. Ishii, "Construction of fluctuation load model and dynamic simulation with LFC control of DC power system and frequency converter interconnection," in *Proc. IEEE/PES Transmiss. Distrib. Conf. Exhib.*, vol. 1, Sep. 2002, pp. 382–387.

[54] C. Hua, J. Lin, and C. Shen, "Implementation of a DSP-controlled photovoltaic system with peak power tracking," *IEEE Trans. Ind. Electron.*, vol. 45, no. 1, pp. 99–107, Feb. 1998.

[55] K. J. Åström, "Theory and applications of adaptive control—A survey," *Automatica*, vol. 19, no. 5, pp. 471–486, Sep. 1983.

[56] Y. Li, Y. Chen, and I. Podlubny, "Stability of fractional-order nonlinear dynamic systems: Lyapunov direct method and generalized Mittag–Leffler stability," *Comput. Math. With Appl.*, vol. 59, no. 5, pp. 1810–1821, Mar. 2010.

[57] M. A. Duarte-Mermoud, N. Aguila-Camacho, J. A. Gallegos, and R. Castro-Linares, "Using general quadratic Lyapunov functions to prove Lyapunov uniform stability for fractional order systems," *Commun. Nonlinear Sci. Numer. Simul.*, vol. 22, nos. 1–3, pp. 650–659, May 2015.

[58] K. J. Åström and B. Wittenmark, *Adaptive Control*. Chelmsford, MA, USA: Courier Corporation, 2013.

[59] Q. Zheng and Z. Gao, "Predictive active disturbance rejection control for processes with time delay," *ISA Trans.*, vol. 53, no. 4, pp. 873–881, Jul. 2014.

[60] S. K. Lakshmanaprabu, M. Elhoseny, and K. Shankar, "Optimal tuning of decentralized fractional order PID controllers for TITO process using equivalent transfer function," *Cognit. Syst. Res.*, vol. 58, pp. 292–303, Dec. 2019.
[61] B. M. Vinagre, I. Podlubny, A. Hernandez, and V. Feliu, "Some approximations of fractional order operators used in control theory and applications," *Fract. Calculus Appl. Anal.*, vol. 3, no. 3, pp. 231–248, 2000.
[62] A. Yazdizadeh, M. H. Ramezani, and E. Hamedrahmat, "Decentralized load frequency control using a new robust optimal MISO PID controller," *Int. J. Electr. Power Energy Syst.*, vol. 35, no. 1, pp. 57–65, Feb. 2012.
[63] Z. A. Obaid, L. M. Cipcigan, L. Abrahim, and M. T. Muhssin, "Frequency control of future power systems: Reviewing and evaluating challenges and new control methods," *J. Modern Power Syst. Clean Energy*, vol. 7, no. 1, pp. 9–25, Jan. 2019.
[64] M. Ahmed, G. Magdy, M. Khamies, and S. Kamel, "Modified TID controller for load frequency control of a two-area interconnected diverse-unit power system," *Int. J. Electr. Power Energy Syst.*, vol. 135, Feb. 2022, Art. no. 107528.

AHMED RAGAB was born in Giza, Egypt, in 1990. He received the bachelor's degree in electric power and machines from the Engineering Faculty, Fayoum University, Egypt, in 2011, and the M.Tech. degree in utilization of electrical energy from the Engineering Faculty, Cairo university, Egypt, in 2017. He was an Automation Engineer in MASS firm, from 2012 to 2014, and a Maintenance Engineer in ZAFRANA wind farm, Egypt, from 2014 to 2017, where he executed many mega projects and designed control and power cabinets in industrial sectors, water and power plant, and oil and gas firms. Since 2017, he has been a TA with the Engineering Mathematics Department, Engineering Faculty, Fayoum University. His research interests include utilization of renewable energy, optimization algorithms, fractional calculus, adaptive control, and control theory.

DALIA ALLAM received the B.Sc., M.Sc., and Ph.D. degrees in electrical power engineering from Cairo University, Egypt. She was certified as a Siemens Trainer in several automation subjects. She was an Ex-Manager of the Automatic Control Unit, Fayoum University, Egypt, where she is currently an Associate Professor with the Department of Electrical Engineering. She has many publications in highly refereed international journals. Her research interests include applications of AI and SI in electrical power engineering, renewable energy, power quality, smart relays and digital protection systems, and automation and process control. She is also a reviewer of many international journals.

AHMED F. ZOBAA (Senior Member, IEEE) received the B.Sc. (Hons), M.Sc., and Ph.D. degrees in electrical power and machines from Cairo University, Egypt, in 1992, 1997, and 2002, respectively, and the Doctoral of Science degree from Brunel University of London, U.K., in 2017. He received his Postgraduate Certificate in Academic Practice from the University of Exeter, U.K., in 2010. He was an Instructor from 1992–1997, a Teaching Assistant from 1997–2002, and an Assistant Professor from 2002–2007 at Cairo University, Egypt. From 2007 to 2010, he was a Senior Lecturer in renewable energy at the University of Exeter, U.K. From 2010 to 2019, he was a Senior Lecturer in power systems at Brunel University of London. He is a Reader in electrical and power engineering and a Member of the Brunel Interdisciplinary Power Systems Research Centre at Brunel University of London. His main areas of expertise include power quality, (marine) renewable energy, smart grids, energy efficiency, and lighting applications. He is the Executive Editor-in-Chief of *Smart Grids and Sustainable Energy Journal*. He is also an Editorial Board member, Editor, Associate Editor, and Editorial Advisory Board member for many international journals. He is a registered Chartered Engineer, Chartered Energy Engineer, European Engineer, and International Professional Engineer. He is also a registered member of the Engineering Council, U.K., the Egypt Syndicate of Engineers, and the Egyptian Society of Engineers. He is a Principal Fellow of the Higher Education Academy, U.K., Fellow of the Institution of Engineering and Technology, Energy Institute, U.K., the Chartered Institution of Building Services Engineers, U.K., the Institution of Mechanical Engineers, U.K., the Royal Society of Arts, U.K., and the African Academy of Sciences.

HAZEM ALI ATTIA received the B.Sc. and M.Sc. degrees in electrical power engineering from Cairo University, Egypt, in 1985 and 1988, respectively, and the M.Sc. and Ph.D. degrees from Arizona University, Tucson, USA, in 1992 and 1993, respectively. He was the Dean of the Engineering Faculty, Fayoum University, Egypt, from 2011 to 2014. He was the Head of the Engineering Mathematics Department, Engineering Faculty, Fayoum University, from 2015 to 2024. He is currently a Professor in engineering mathematics with Fayoum University; and a Visitor Scholar in many universities in Egypt, Oman, and Saudi Arabia. His research interests include heat transfer, rigid bodies, engineering mathematics, fluid mechanics, mechanical engineering, and mathematical physics. He received the Excellence Awards in Scientific Research from many official firms in Egypt and Italy. He is a Reviewer of many reputed journals, such as IEEE Magnetic Letters, *Entropy*, MDPI Publishing, *International Journal of Applied and Computational Mathematics*. He is a member of the editorial board of many international engineering journals, such as *Kragujevac Journal of Science*, *Trends on Applied Sciences Research*, and *Asian Journal of Mathematics and Statistics*.